

AD-A071 878 GENERAL MOTORS CORP INDIANAPOLIS IND DETROIT DIESEL --ETC F/G 21/5  
THE EFFECT OF INTERBLADE PHASE ANGLE AND SOLIDITY ON THE TIME-V--ETC(U)  
JUN 79 R R ALLRAN F49620-78-C-0070

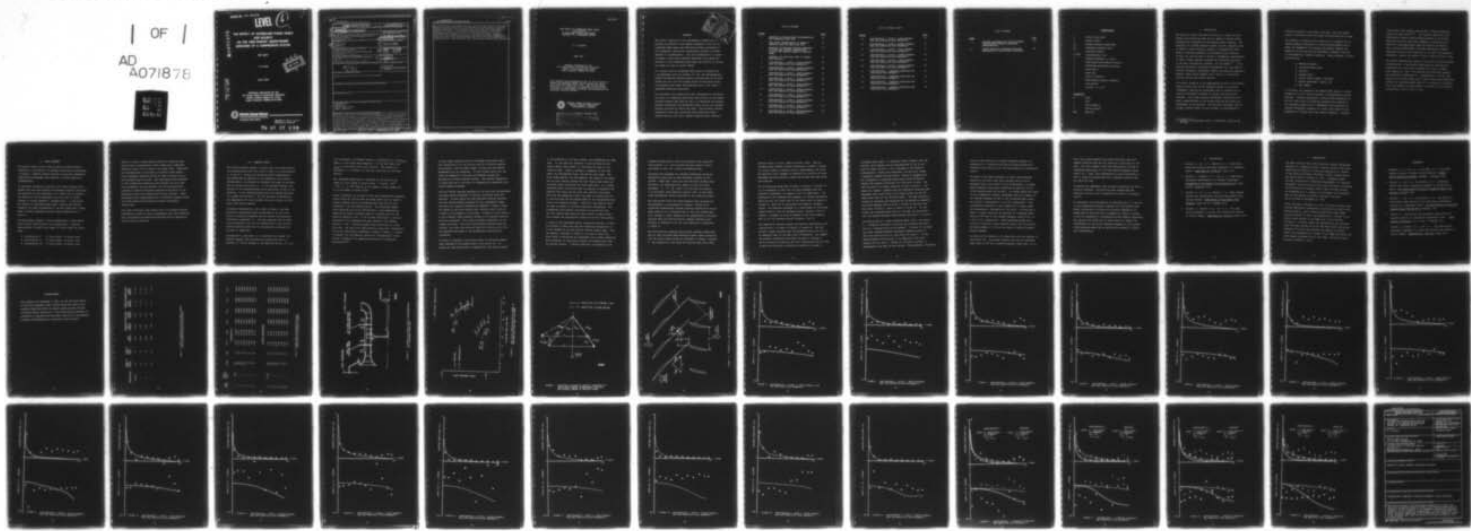
UNCLASSIFIED

DDA-EDR-9930

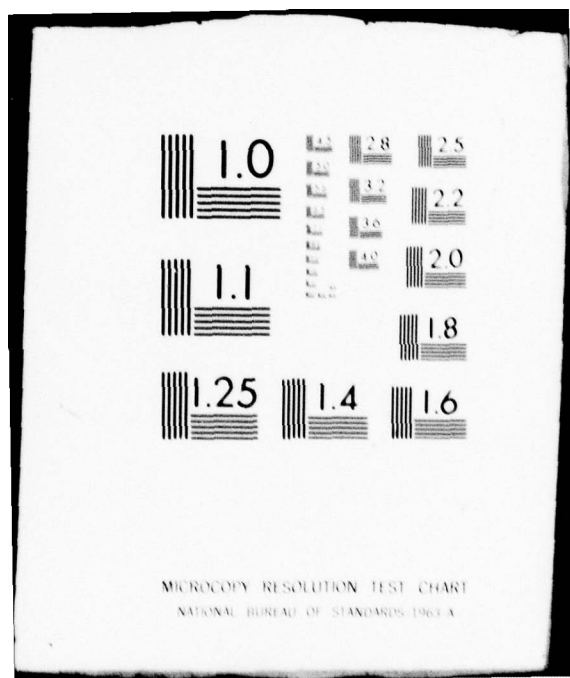
AFOSR-TR-79-0853

NL

| OF |  
AD  
A071878



END  
DATE  
FILMED  
8-79  
DDC



AFOSR-TR- 79-0853

LEVEL

Q

ADA 071878

THE EFFECT OF INTERBLADE PHASE ANGLE  
AND SOLIDITY  
ON THE TIME-VARIANT AERODYNAMIC  
RESPONSE OF A COMPRESSOR STATOR

EDR 9930

R. R. Allran



FILE COPY

June 1979

Research Sponsored by the  
Air Force Office of Scientific Research  
(AFSC) United States Air Force  
under Contract F49620-78-C-0070



**Detroit Diesel Allison**  
Division of General Motors Corporation

Indianapolis, Indiana 46206

Approved for public release;  
distribution unlimited.

79 07 27 030

UNCLASSIFIED

SECURITY CLASSIFICATION OF THIS PAGE (When Data Entered)

| REPORT DOCUMENTATION PAGE  |                       | READ INSTRUCTIONS BEFORE COMPLETING FORM   |
|--|-----------------------|--|
| 1. REPORT NUMBER<br>⑧ AFOSR-TR-79-0853   | 2. GOVT ACCESSION NO. | 3. RECIPIENT'S CATALOG NUMBER  |
| 4. TITLE (and Subtitle)<br>⑥ THE EFFECT OF INTERBLADE PHASE ANGLE AND SOLIDITY ON THE TIME-VARIANT AERODYNAMIC RESPONSE OF A COMPRESSOR STATOR.  |                       | 5. TYPE OF REPORT & PERIOD COVERED<br>⑨ INTERIM Rept.<br>1 May 1978 - 1 May 1979           |
| 6. AUTHOR(s)<br>⑩ R. R. ALLRAN   |                       | 7. CONTRACT OR GRANT NUMBER(s)<br>⑪ F49620-78-C-0070                                       |
| 8. PERFORMING ORGANIZATION NAME AND ADDRESS<br>DETROIT DIESEL ALLISON<br>PO BOX 894/DIVISION OF GENERAL MOTORS CORP<br>INDIANAPOLIS, IN 40206  |                       | 9. PROGRAM ELEMENT, PROJECT, TASK AREA & WORK UNIT NUMBERS<br>⑫ 2307A4<br>61102F<br>⑬ 19A4 |
| 10. CONTROLLING OFFICE NAME AND ADDRESS<br>AIR FORCE OFFICE OF SCIENTIFIC RESEARCH/NA<br>BLDG 410<br>BOLLING AIR FORCE BASE, D C 20332   |                       | 11. REPORT DATE<br>⑭ Jun 1979  |
| 12. MONITORING AGENCY NAME & ADDRESS (if different from Controlling Office)<br>⑮ 55p.  |                       | 13. NUMBER OF PAGES<br>50  |
| 14. SECURITY CLASS. (of this report)   |                       | 15. SECURITY CLASS. (of this report)<br>UNCLASSIFIED                                       |
| 16. DISTRIBUTION STATEMENT (of this Report)<br><br>Approved for public release; distribution unlimited.  |                       | 17. DECLASSIFICATION/DOWNGRADING SCHEDULE  |
| 18. DISTRIBUTION STATEMENT (of the abstract entered in Block 20, if different from Report)   |                       |  |
| 19. SUPPLEMENTARY NOTES  |                       |  |
| 20. KEY WORDS (Continue on reverse side if necessary and identify by block number)<br>TURBOMACHINERY<br>COMPRESSORS<br>UNSTEADY AERODYNAMICS<br>FORCED VIBRATIONS  |                       |  |
| 21. ABSTRACT (Continue on reverse side if necessary and identify by block number)<br>The overall objective of this experimental program was to quantify the effects of the reduced frequency as well as the interblade phase angle and associated solidity variations on the fundamental time-variant aerodynamics relevant to forced response in turbomachinery. This was accomplished in a large, low speed, single-stage research compressor which permitted variation of the interblade phase angle and solidity by varying the number of rotor to stator blades. A single value of interblade phase angle, 36 degrees and a corresponding value of solidity of .758, the aerodynamically induced fluctuating surface pressure |                       |  |

UNCLASSIFIED

SECURITY CLASSIFICATION OF THIS PAGE(When Data Entered)

distributions on the downstream vane row, with the primary source of excitation being the upstream rotor wakes, were measured over a wide range of compressor operating conditions. The individual vane surface data were investigated to determine the effect of interblade phase angle and solidity on the overall unsteady pressure magnitude as well as to determine the dynamic pressure coefficient and aerodynamic phase lag for the unsteady pressure differential across the vanes. The unsteady pressure differential data were correlated with predictions from a state-of-the-art flat plate cascade transverse gust analysis.

UNCLASSIFIED

THE EFFECT OF INTERBLADE PHASE ANGLE  
AND SOLIDITY  
ON THE TIME-VARIANT AERODYNAMIC  
RESPONSE OF A COMPRESSOR STATOR

R. R. ALLRAN

JUNE 1979

Research Sponsored by the  
Air Force Office of Scientific Research  
(AFSC) United States Air Force  
under Contract F49620-78-C-0070

This research was sponsored by the Air Force Office of Scientific Research (AFSC) United States Air Force, under Contract F49620-78-C-0070. The United States Government is authorized to reproduce and distribute reprints for governmental purposes notwithstanding any copyright notation hereon.



DETROIT DIESEL ALLISON DIVISION  
GENERAL MOTORS CORPORATION  
INDIANAPOLIS, INDIANA

AIR FORCE OFFICE OF SCIENTIFIC RESEARCH (AFSC)  
NOTICE OF TRANSMITTAL TO DDC  
This technical report has been reviewed and is  
approved for public release IAW AFN 190-12 (7b).  
Distribution is unlimited.  
A. D. BLOSE  
Technical Information Officer

|               |                         |
|---------------|-------------------------|
| Accession For | NTIS GRAAL              |
| DDC TAB       | Unannounced             |
| Justification | By                      |
| Distribution  | Avalability Codes       |
| Dist          | Avail and/or<br>special |

## ABSTRACT

The overall objective of this experimental program was to quantify the effects of the reduced frequency as well as the interblade phase angle and associated solidity variations on the fundamental time-variant aerodynamics relevant to forced response in turbomachinery. This was accomplished in a large, low speed, single-stage research compressor which permitted variation of the interblade phase angle and solidity by varying the number of rotor to stator blades.

At a single value of interblade phase angle, 36 degrees and a corresponding value of solidity of .758, the aerodynamically induced fluctuating surface pressure distributions on the downstream vane row, with the primary source of excitation being the upstream rotor wakes, were measured over a wide range of compressor operating conditions.

The individual vane surface data were investigated to determine the effect of interblade phase angle and solidity on the overall unsteady pressure magnitude as well as to determine the dynamic pressure coefficient and aerodynamic phase lag for the unsteady pressure differential across the vanes. The unsteady pressure differential data were correlated with predictions from a state-of-the-art flat plate cascade transverse gust analysis.

## LIST OF FIGURES

| <u>FIGURE</u> |  | <u>PAGE</u> |
|---------------|--|-------------|
| 1             | SCHEMATIC OF STEADY-STATE INSTRUMENTATION AND COMPRESSOR FLOW PATH   | 21          |
| 2             | DATA POINT IDENTIFICATION IN TERMS OF PRESSURE RATIO AND MASS FLOW RATE  | 22          |
| 3             | REDUCTION IN RELATIVE VELOCITY GENERATED BY BLADE WAKE CREATES CORRESPONDING VELOCITY AND ANGULAR CHANGE IN ABSOLUTE FRAME | 23          |
| 4             | SCHEMATIC OF FLOW FIELD USED IN DYNAMIC DATA ANALYSIS  | 24          |
| 5             | CONFIGURATION I, POINT 1, FIRST HARMONIC DATA AND PREDICTION FROM REFERENCE 4  | 25          |
| 6             | CONFIGURATION I, POINT 1, SECOND HARMONIC DATA AND PREDICTION FROM REFERENCE 4   | 26          |
| 7             | CONFIGURATION I, POINT 2, FIRST HARMONIC DATA AND PREDICTION FROM REFERENCE 4  | 27          |
| 8             | CONFIGURATION I, POINT 2, SECOND HARMONIC DATA AND PREDICTION FROM REFERENCE 4   | 28          |
| 9             | CONFIGURATION I, POINT 3, FIRST HARMONIC DATA AND PREDICTION FROM REFERENCE 4  | 29          |
| 10            | CONFIGURATION I, POINT 3, SECOND HARMONIC DATA AND PREDICTION FROM REFERENCE 4   | 30          |
| 11            | CONFIGURATION I, POINT 4, FIRST HARMONIC DATA AND PREDICTION FROM REFERENCE 4  | 31          |
| 12            | CONFIGURATION I, POINT 4, SECOND HARMONIC DATA AND PREDICTION FROM REFERENCE 4   | 32          |
| 13            | CONFIGURATION I, POINT 5, FIRST HARMONIC DATA AND PREDICTION FROM REFERENCE 4  | 33          |
| 14            | CONFIGURATION I, POINT 5, SECOND HARMONIC DATA AND PREDICTION FROM REFERENCE 4   | 34          |

LIST OF FIGURES (CONT.)

| <u>FIGURE</u> |  | <u>PAGE</u> |
|---------------|--|-------------|
| 15            | CONFIGURATION I, POINT 6, FIRST HARMONIC DATA AND PREDICTION FROM REFERENCE 4  | 35          |
| 16            | CONFIGURATION I, POINT 6, SECOND HARMONIC DATA AND PREDICTION FROM REFERENCE 4 | 36          |
| 17            | CONFIGURATION I, POINT 7, FIRST HARMONIC DATA AND PREDICTION FROM REFERENCE 4  | 37          |
| 18            | CONFIGURATION I, POINT 7, SECOND HARMONIC DATA AND PREDICTION FROM REFERENCE 4 | 38          |
| 19            | CONFIGURATION I, POINT 8, FIRST HARMONIC DATA AND PREDICTION FROM REFERENCE 4  | 39          |
| 20            | CONFIGURATION I, POINT 8, SECOND HARMONIC DATA AND PREDICTION FROM REFERENCE 4 | 40          |
| 21            | CONFIGURATION I - BASELINE COMPARISON AND PREDICTION FROM REFERENCE 4          | 41          |
| 22            | CONFIGURATION I - BASELINE COMPARISON AND PREDICTION FROM REFERENCE 4          | 42          |
| 23            | CONFIGURATION I - BASELINE COMPARISON AND PREDICTION FROM REFERENCE 4          | 43          |
| 24            | CONFIGURATION I - BASELINE COMPARISON AND PREDICTION FROM REFERENCE 4          | 44          |

LIST OF TABLES

| <u>TABLE</u> |  | <u>PAGE</u> |
|--------------|--|-------------|
| I            | RELEVANT PARAMETERS FOR FOUR LOW-SPEED,<br>SINGLE-STAGE, RESEARCH COMPRESSOR<br>CONFIGURATIONS | 19          |
| II           | STEADY-STATE DATA IDENTIFICATION AND<br>DESCRIPTION OF TIME-VARIANT PARAMETERS                 | 20          |

### NOMENCLATURE

|                          |  |
|--------------------------|--|
| b                        | Airfoil semi-chord                     |
| c                        | Airfoil chord                          |
| $C_p$                    | Dynamic pressure coefficient           |
| $R_c$                    | Compressor pressure ratio              |
| v                        | Absolute velocity                      |
| $w \sqrt{\theta/\delta}$ | Corrected mass flow                    |
| k                        | Reduced frequency ( $k = \omega b/V$ ) |
| u                        | Longitudinal perturbation velocity     |
| v                        | Transverse perturbation velocity       |
| $\beta$                  | Inlet angle                            |
| $\phi$                   | Phase lag                              |
| $\rho$                   | Inlet air density                      |
| $\omega$                 | Blade passing angular frequency        |
| s                        | Vane spacing                           |
| $\sigma$                 | Solidity ( $\sigma = C/S$ )            |

### SUBSCRIPTS

|     |                 |
|-----|-----------------|
| B   | Blade           |
| V   | Vane            |
| 1   | First Harmonic  |
| 2   | Second Harmonic |
| ABS | Absolute        |

## I. INTRODUCTION

The failure of rotor and stator airfoils as a result of aerodynamic excitations has been and yet remains a serious design consideration throughout the gas turbine engine industry. The discovery of a forced response problem, and the subsequent need to affect a viable solution, results in increased unit cost, delays in delivery schedules and decreased flight readiness. As early as 1955 the need to develop a fundamental understanding of these "forced response" problems was recognized and noted in the open literature by Whitmore, Lull and Adams<sup>(1)</sup>. In the ensuing time period significant advancements have been made in solution techniques, aerodynamic theory and computing capability. However, today forced response still ranks as a significant problem area for gas turbine engines.

The overall objective of the experimental portion of the Detroit Diesel Allison (DDA) forced response program is to provide fundamental time-variant aerodynamic data to validate and to indicate refinements necessary to current state-of-the-art analyses. This unique unsteady aerodynamic cascade data will lead to modifications of the current analyses and direct the development of new analyses. The unsteady aerodynamic data of primary interest herein is that relevant to aerodynamically

---

(1) Numbers in parentheses refer to references listed at end of test.

induced vibrations in stationary vane rows, with the primary source of excitation being the wakes from upstream rotor blades.

The approach to achieving this objective is to measure the unsteady pressure distribution in controlled experiments which model the fundamental flow physics and thereby identify and quantify the key time-variant aerodynamic parameters relevant to aerodynamically induced vibrations. These parameters include the following:

- Reduced frequency,
- Interblade phase angle,
- Solidity,
- Stagger angle,
- Airfoil shape (camber, thickness),
- Steady aerodynamic loading, and
- Mach number.

In the above list experience has demonstrated several of these parameters to have a major influence on aerodynamically forced response. Previous experimental programs under sponsorship of the Air Force Office of Scientific Research have resulted in the successful acquisition of fundamental data regarding the unsteady aerodynamic response of a stator vane where the key parameters of interest have been reduced frequency, incidence,

rotor-stator axial spacing, wake profile, steady aerodynamic loading and Mach number<sup>(2,3)</sup>. The specific objective of the experimental research program reported herein is to provide additional data with particular emphasis on quantifying the effects of interblade phase angle and solidity variations. This is being accomplished in the DDA large-scale, research compressor facility with variations in the above key parameters achieved by varying the number of rotor blades and stator vanes.

The results reported here pertain to the first of three proposed configurations. A previously tested baseline configuration consisted of 42 rotors and 40 stators at a rotor to stator axial spacing of .4305. The baseline data have been reported and discussed in Reference (3). Configuration I of this task consists of 42 rotor blades and 20 stator vanes which effectively doubles the interblade phase angle to 36 (relative to the baseline) and reduces the vane solidity to one-half of its baseline configuration value (1.516 to .758).

## II. WORK STATEMENT

The Detroit Diesel Allison (DDA) Division of General Motors Corporation is furnishing all necessary facilities and personnel to conduct a research program directed at obtaining fundamental time-variant aerodynamic data relevant to forced response in turbomachinery.

An experiment directed at obtaining this unique unsteady aerodynamic data has been designed and necessary hardware fabricated. The objective of this experiment is to obtain data to quantify the effects of the key parameters over the range of values relevant to forced response in turbomachinery. In particular, the effects of interblade phase angle, solidity and reduced frequency are being investigated in the DDA large-scale, single-stage, research compressor facility shown schematically in Figure 1.

The experimental program is being accomplished in three phases which involve three distinct rig configurations. These are characterized in terms of the number of rotor blades and stator vanes.

- Configuration I: 42 rotor blades 20 stator vanes
- Configuration II: 21 rotor blades 20 stator vanes
- Configuration III: 21 rotor blades 40 stator vanes

Testing in each of these phases consists of obtaining time-variant data at approximately eight steady-state compressor operating points, four on each of two speed lines. Sufficient rig instrumentation is provided to ascertain these steady-state compressor operating points in terms of pressure ratio and corrected mass flow rate. The time-variant data obtained at each steady-state operating point defines the rotor wake (the aerodynamic forcing function) and the resulting aerodynamically induced fluctuating pressure distribution on the downstream stator vane pressure and suction surfaces. These measurements are accomplished with a calibrated crosswire probe and flush mounted Kulite dynamic pressure transducers, respectively.

From these individual vane surface data, the unsteady pressure differential across the vane is determined, and this difference data correlated with predictions obtained from an appropriate state-of-the-art analysis.

### III. RESEARCH STATUS

The current research program is broken down into three distinct rig configurations which are listed in Table I as Configuration I, II and III. During this reporting period Configuration I was tested and the results will be reported in this section. Configuration I is directed at extending the range of available data to include variations in: (1) the reduced frequency and solidity at an interblade phase angle equivalent to that of the baseline; (2) the interblade phase angle and reduced frequency at a common vane solidity. This was achieved by building-up the compressor with the 42 bladed rotor and a stator row with every other stator removed.

A baseline configuration, also listed in Table I, has been previously investigated under sponsorship of the Air Force Office of Scientific Research and the results are thoroughly discussed in Reference (3). The data obtained from the baseline configuration will not be repeated here in its entirety; however selected points will be discussed and presented for the sake of comparison.

Configuration I duplicates, at a specified rotor speed, the reduced frequency for the baseline configuration but at a solidity of .758 as compared to the baseline solidity of 1.516.

For the stators, the reduced frequency is defined as  $k = \omega C / 2V_{\text{axial}}$  where  $\omega$  is the blade pass frequency,  $C$  is the vane chord, and  $V_{\text{axial}}$  is the stator inlet axial velocity. The solidity is defined as  $\sigma = C/S$  where  $C$  is the vane chord and  $S$  is the vane spacing.

The interblade phase angle is specified by the ratio of the number of rotor blades to stator vanes:  $\theta = N_B / N_V \cdot 360^\circ$ ,  $-180^\circ \leq \theta \leq +180^\circ$  where  $N_B$  is the number of rotor blades and  $N_V$  is the number of stator vanes.

Figure 2 presents the location of the eight steady-state operating points along the 70% and 100% corrected speed lines in terms of overall pressure ratio and corrected mass flow rate for Configuration I and the baseline points. The particular steady-state operating points for Configuration I were determined by matching the stator incidence angle at a similar point on the baseline operating line. It can be seen from Figure 2 that the operation of the compressor has been altered at the reduced solidity (.758), a similar pressure ratio occurring at a lower flow rate. The data point identification along with a description of the key time-variant parameters is shown in Table II. Points 1 through 8 are the operating points for Configuration I while points 9 through 16 are comparative points for the baseline Configuration<sup>(3)</sup>.

At each steady operating point an averaged time-variant data set, consisting of the two hot-wire and the 22 Kulite signals, are obtained. Each of these signals is digitized and Fourier decomposed into its harmonics. In this investigation only the first two harmonics of the data are examined through the entirety of the data analysis process. The reduced frequencies of these data are in the range of turbomachinery experience with forced response problems.

From the Fourier analyses performed on the data both the magnitude and phase angles referenced to the data initiation pulse are obtained. To then relate the wake generated velocity profiles with the surface dynamic pressures on the instrumented vanes, the rotor exit velocity triangles are examined. Figure 3 shows the change in the rotor relative exit velocity which occurs as a result of the presence of the blade. A deficit in the velocity in this relative frame creates a change in the absolute velocity vector as indicated. This velocity change is measured via the crossed hot-wires. From this instantaneous absolute angle and velocity, the rotor exit relative angle and velocity as well as the magnitude and phase of the perturbation quantities are determined.

As Figure 4 indicates, the hot-wire probe is positioned immediately upstream of the leading edge of the stator row. To relate the time based events as measured by this hot-wire probe

to the pressures on the vane surfaces, the assumptions are made that: (1) the wakes are identical at the hot-wire and the stator leading edge planes; (2) the wakes are fixed in the relative frame. Figure 4 presents a schematic of the rotor wakes, the instrumented vanes, and the hot-wire probe. The rotor blade spacing, the vane spacing, the length of the probe, and the axial spacing between the vane leading edge plane and the probe holder centerline are known quantities. At a steady operating point the hot-wire data is analyzed to determine the absolute flow angle and the rotor exit relative flow angle. Using the two assumptions noted, the wake is located relative to the hot-wires and the leading edges of the instrumented vane suction and pressure surfaces. From this, the times at which the wake is present at various locations is determined. The incremented times between occurrences at the hot-wire and the vane leading edge plane are then related to phase differences between the perturbation velocities and the vane surface.

To simplify the experiment-theory correlation process, the data is adjusted in phase such that the transverse perturbation is at zero degrees at the vane suction surface leading edge. From the geometry indicated in Figure 4, the time at which this would occur is calculated and transposed into a phase difference. This difference is then used to adjust the pressure data from the suction surface. A similar operation is performed on the

pressure surface data so that the surfaces of the vanes are time related; i.e., time relating the data results in data equivalent to that for a single instrumented vane.

Following this procedure the pressure differences across an equivalent single vane at each transducer location is calculated. These data, along with the individual surface pressure data, are normalized with respect to the inlet flow parameter:  $(\rho \cdot v^2 \cdot \frac{v}{V})$  where  $\rho$  is the inlet air density,  $v$  is the stator inlet absolute velocity, and  $v$  is the transverse perturbation velocity measured by the cross-wire probe.

The time-variant first and second harmonic data obtained for Configuration I are presented in Figures 5 through 20 as normalized dimensionless unsteady pressure coefficients and its phase relation to a transverse gust at the vane leading edge. Also included in these figures are the compressible predictions obtained from the state-of-the-art cascade transverse gust analysis of Reference 4 for the flow conditions as specified in Table II.

The high negative incidence angle dynamic pressure coefficient data at 100% corrected speed generally exhibit good correlation over the entire blade surface as indicated in Figures 5 through 8. The exception to that being the trailing edge value where

the data attain a finite, albeit non-zero, value. The low incidence angle dynamic pressure coefficient, Figures 9 through 12, attains almost a constant value at approximately 10% chord and exhibits little tendency to decrease as a function of chord. The phase lag also exhibits a sharp dip at about the same chordwise location.

The 70% corrected speed data is shown in Figures 13 through 20. It is interesting to note that the wave phenomena that was reported in Reference (5) appears at the 70% speed point. The dominance of the convected wave appears as a rapidly decreasing phase lag over the latter half of the stator vane in Figures 13 through 16, which are at relatively high negative incidence angles. The dominance decreases to a large extent on the second harmonic data at the low incidence points, Figures 18 and 20; however, it appears to still be present in the first harmonic data at the low incidence points, Figures 17 and 19.

The comparative relation between the baseline configuration and Configuration I is shown in Figures 21 through 24. The comparison is made realizing that the parameters which are felt to be important have not yet been fully investigated. For example, the pressure coefficient and phase lag shown in Figures 21 and 22 for both the baseline and first configuration may be used to show the difference or similarity caused by a change in

interblade phase angle. It should be noted, however, that the solidity ratio between the two configurations is two to one with the higher solidity (1.516) belonging to the baseline configuration. Noting this difference, one may still assess a similarity between the two builds. Figure 21 suggests that for a doubling of interblade phase angle little difference between the pressure coefficient for each build is seen. The data for point 9 is almost identical to that of point 1. The phase lag, however, suggests that the dominating convected wave phenomena occurs much later on the blade surface for the  $36^\circ$  phase angle than for the  $18^\circ$  phase angle. The same conclusion concerning convected wave dominance may be reached by comparing the second harmonic data of point 9 to that of the first harmonic data of point 1, which is shown in Figure 22. In this figure the interblade phase angle is the same for both points with the reduced frequency being doubled from point 1 to point 9.

Considering data at a lower incidence angle, point 3 and point 11, a different conclusion concerning the existence and dominance of a convected wave can be reached. In Figure 23 the phase lag shows a marked decrease (increasing negative value) at about 40% chord for point 11 and little for point 3. If the second harmonic data of point 11 is compared to the first harmonic data of point 3, Figure 24, the phase lag data is approximately the same for both points. The conclusion, therefore,

would be that doubling the reduced frequency prevents the appearance of a convected wave down the blade surface with incidence angle entering into the relationship as a controlling factor.

The point in the above discussion is that a more detailed analysis of the data, both that available and yet to be generated during the course of this investigation, is needed before adequate conclusions concerning the behavior of the forced response model can be made. To further extend the range of this fundamental unsteady aerodynamic data with respect to the reduced frequency as well as the interblade phase angle and solidity, Configuration II will be investigated. This configuration features 21 rotor blades and 20 stator vanes, and necessitates a rebalancing of the rotor. As indicated in Table I, dynamic data will be obtained for interblade phase angles of  $18^\circ$  and  $36^\circ$  and reduced frequency values from 3 to 5 and 6 to 10 respectively. These interblade phase angle values are identical to the baseline values, but the solidity has been reduced to 0.758 and the range of reduced frequency values extended.

Configuration II features a 21 bladed rotor and the complete 40 vane stator row. The second harmonic data has an interblade phase angle of  $18^\circ$  and a reduced frequency range from 6 to 10.

Thus, this second harmonic data should duplicate the first harmonic baseline data and will serve as a valid check on the data. The first harmonic data from Configuration III has an interblade phase angle of  $-171^\circ$  and reduced frequency values from 3 to 5. Thus, this configuration is very significant in that it acquires unsteady data for a backward traveling wave for the first time.

At present the compressor rotor has been rebalanced with the 21 airfoils installed. Rig build has been accomplished and electronic set-up is now in progress for testing of Configuration II.

In conclusion, the investigation of Configurations I, II and III in this experimental program, together with the baseline data should significantly increase the available fundamental unsteady data to much more fully encompass the range of interest of the key parameters of turbomachine forced response experience. The analysis and correlation of these data will enhance the understanding of the forced response phenomena so that present forced response models may be modified and updated to reflect this understanding.

#### IV. PUBLICATIONS

1. Fleeter, S., Jay, R. L., Bennett, W. A., "Rotor Wake Generated Unsteady Aerodynamic Response of a Compressor Stator", ASME Paper No. 78-GT-112, April 1978.
2. Fleeter, S., Bennett, W. A., Jay, R. L., "Time-Variant Aerodynamic Measurements in a Research Compressor", Proceedings of the Dynamic Flow Conference 1978, pages 279-285, September 1978.
3. Fleeter, S., Jay, R. L., Bennett, W. A., "Wake Induced Time-Variant Aerodynamics Including Rotor-Stator Axial Spacing Effects", ASME Journal of Non-Steady Fluid Dynamics, pages 147-163, December 1978.
4. Fleeter, S., Bennett, W. A., Jay, R. L., "The Time-Variant Response of a Stator Row Including the Effects of Airfoil Camber", ASME Paper No. 79-GT-110, March 1979.

## V. INTERACTIONS

The paper entitled "Rotor Wake Generated Unsteady Aerodynamic Response of a Compressor Stator" covering research done under AFOSR contract F44620-74-C-0065 was presented by S. Fleeter at the Annual Gas Turbine Conference, London, England during the week of April 9 through 13, 1978. A companion paper entitled "Time-Variant Aerodynamic Measurements in a Research Compressor" covering the particular data acquisition techniques utilized during the research effort under the same contract was presented by W. A. Bennett at the Dynamic Flow Conference held at John Hopkins University, Baltimore, Maryland during the week of September 18, 1978.

During the week of December 10, 1978, the paper entitled "Wake Induced Time-Variant Aerodynamics Including Rotor-Stator Axial Spacing Effects", which covered research done under AFOSR contract F49620-77-C-0024, was presented by S. Fleeter at the Winter Annual Meeting of the ASME held in San Francisco, California. A similar paper that expanded upon data obtained under the same contract entitled "The Time-Variant Aerodynamic Response of a Stator Row Including the Effects of Airfoil Camber" was presented by S. Fleeter at the ASME Gas Turbine and Solar Energy Conference held at San Diego, California during the week of March 12, 1979.

## REFERENCES

1. Whitmore, J. M., Lull, W. R., and Adams, M. D., "How Sound Affects Vibration in Modern Aircraft Engines", General Motors Engineering Journal, November - December, 1955.
2. Fleeter, S., Jay, R. L., and Bennett, W. A., "Compressor Stator Time-Variant Aerodynamic Response to Upstream Rotor Wakes", Air Force Office of Scientific Research Report, DDA EDR 9005, November 1976.
3. Fleeter, S., Jay, R. L., and Bennett, W. A., "The Effect of Rotor-Stator Axial Spacing on the Time-Variant Aerodynamic Response of a Compressor Stator", Air Force Office of Scientific Research Report DDA EDR 9379, December, 1977.
4. Fleeter, S., "Fluctuating Lift and Moment Coefficients for Cascaded Airfoils in a Nonuniform Compressible Flow". AIAA Journal of Aircraft, Vol. 10, No. 2, February 1973.
5. Fleeter, S., Bennett, W. A., Jay, R. L., "The Time Variant Aerodynamic Response of a Stator Row Including the Effects of Airfoil Camber", ASME Paper No. 79-GT-110, March 1979.

#### **ACKNOWLEDGMENT**

This research was sponsored, in part, by the Air Force Office of Scientific Research (AFSC) United States Air Force, under Contract F49620-78-C-0070 to Detroit Diesel Allison Division of General Motors Corporation. The United States Government is authorized to reproduce and distribute reprints for governmental purposes notwithstanding any copyright notation hereon.

| CONFIGURATION | NUMBER OF<br>ROTOR<br>BLADES | NUMBER OF<br>STATOR<br>VANES | VANE<br>SOLIDITY | INTERBLADE PHASE ANGLE |                    |          | REDUCED FREQUENCY RANGE |                    |
|---------------|------------------------------|------------------------------|------------------|------------------------|--------------------|----------|-------------------------|--------------------|
|               |                              |                              |                  | FIRST<br>HARMONIC      | SECOND<br>HARMONIC | HARMONIC | FIRST<br>HARMONIC       | SECOND<br>HARMONIC |
| Baseline      | 42                           | 40                           | 1.516            | + 18°                  | + 36°              |          | 6 - 10                  | 12 - 20            |
| 1             | 42                           | 20                           | 0.758            | + 36°                  | + 72°              |          | 6 - 10                  | 12 - 20            |
| 2             | 21                           | 20                           | 0.758            | + 18°                  | + 36°              |          | 3 - 5                   | 6 - 10             |
| 3             | 21                           | 40                           | 1.516            | - 171°                 | + 18°              |          | 3 - 5                   | 6 - 10             |

TABLE I. RELEVANT PARAMETERS FOR FOUR LOW-SPEED, SINGLE-STAGE, RESEARCH COMPRESSOR CONFIGURATIONS.

| DATA POINT      | AXIAL SPACING RATIO | % SPEED | $\beta_{ABS}$ | $K_1 AX$ | $K_2 AX$ | $v/v)_1$ | $u/v)_1$ | $v/v)_2$ | $u/v)_2$ |
|-----------------|---------------------|---------|---------------|----------|----------|----------|----------|----------|----------|
| CONFIGURATION 1 |                     |         |               |          |          |          |          |          |          |
| 1               | .4305               | 100     | 25            | 6.418    | 12.836   | .04911   | .02785   | .04899   | .02735   |
| 2               | "                   | 100     | 29            | 6.736    | 13.472   | .05055   | .02686   | .04984   | .02607   |
| 3               | "                   | 100     | 33            | 7.517    | 15.034   | .06457   | .02770   | .06024   | .02468   |
| 4               | "                   | 100     | 36            | 8.339    | 16.678   | .14112   | .04760   | .11590   | .03119   |
| 5               | "                   | 70      | 24            | 6.423    | 12.846   | .05145   | .02841   | .05257   | .02998   |
| 6               | "                   | 70      | 27            | 6.642    | 13.284   | .05490   | .02912   | .05390   | .02765   |
| 7               | "                   | 70      | 32            | 7.422    | 14.844   | .07218   | .02962   | .06679   | .02590   |
| 8               | "                   | 70      | 36            | 8.086    | 16.172   | .12857   | .03835   | .10752   | .02519   |

BASELINE CONFIGURATION

|    |        |     |    |       |       |        |        |        |        |
|----|--------|-----|----|-------|-------|--------|--------|--------|--------|
| 9  | 0.4305 | 100 | 25 | 6.95  | 13.90 | .03148 | .01973 | .03203 | .01583 |
| 10 | "      | 100 | 28 | 7.27  | 14.54 | .03306 | .01845 | .03452 | .01556 |
| 11 | "      | 100 | 33 | 8.96  | 17.92 | .07811 | .02499 | .06258 | .01813 |
| 12 | "      | 100 | 36 | 10.05 | 20.10 | .10798 | .01652 | .07397 | .00754 |
| 13 | "      | 70  | 25 | 6.95  | 13.90 | .03388 | .02602 | .03622 | .01863 |
| 14 | "      | 70  | 28 | 7.40  | 14.80 | .03630 | .02360 | .03826 | .01891 |
| 15 | "      | 70  | 33 | 8.91  | 17.82 | .07803 | .03156 | .06462 | .02419 |
| 16 | "      | 70  | 36 | 9.82  | 19.64 | .12118 | .02614 | .08612 | .01381 |

TABLE II. STEADY-STATE DATA IDENTIFICATION AND DESCRIPTION OF TIME-VARIANT PARAMETERS

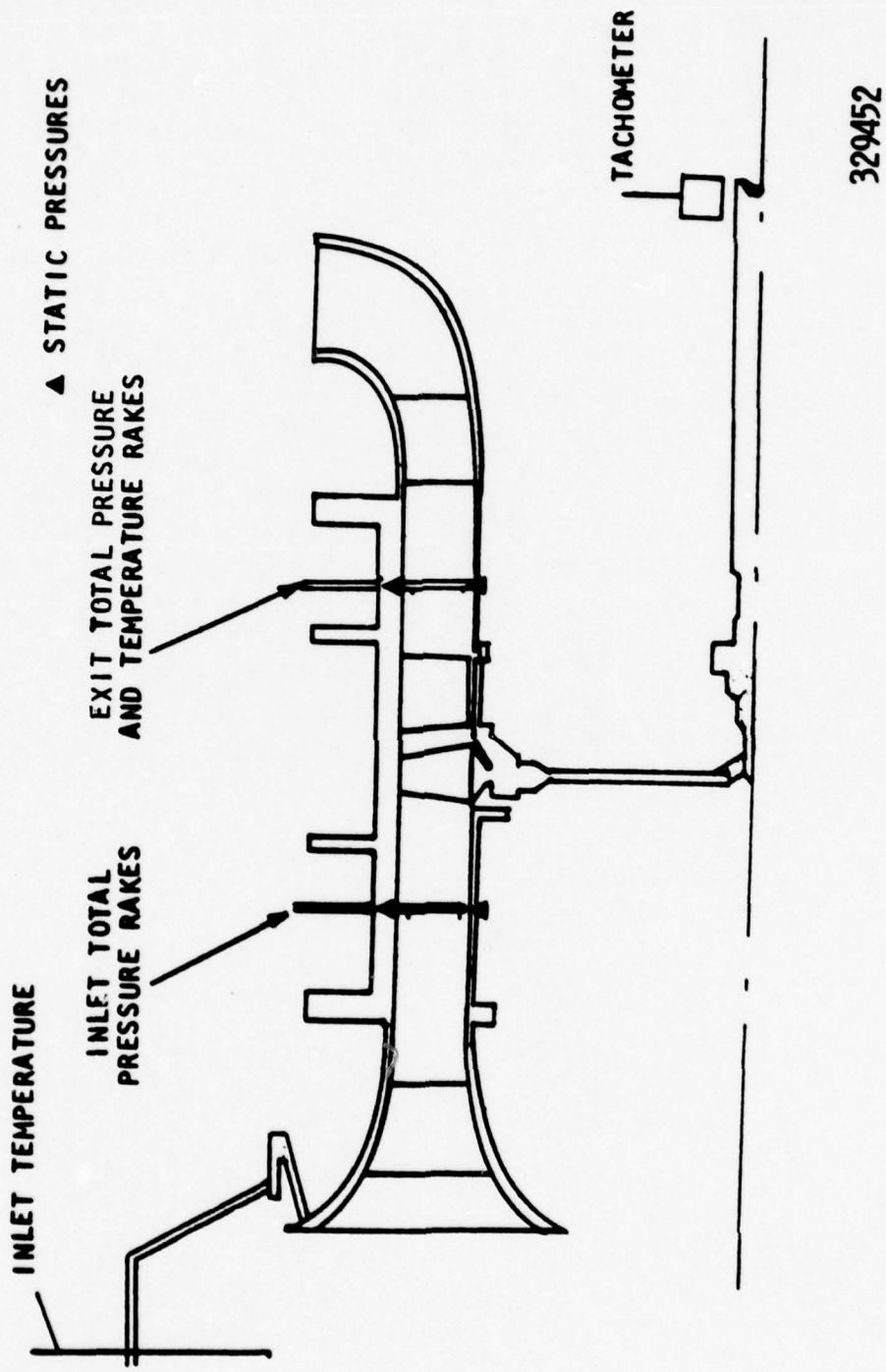


FIGURE 1. SCHEMATIC OF STEADY-STATE INSTRUMENTATION  
AND COMPRESSOR FLOW PATH

( ) DATA POINT IDENTIFICATION

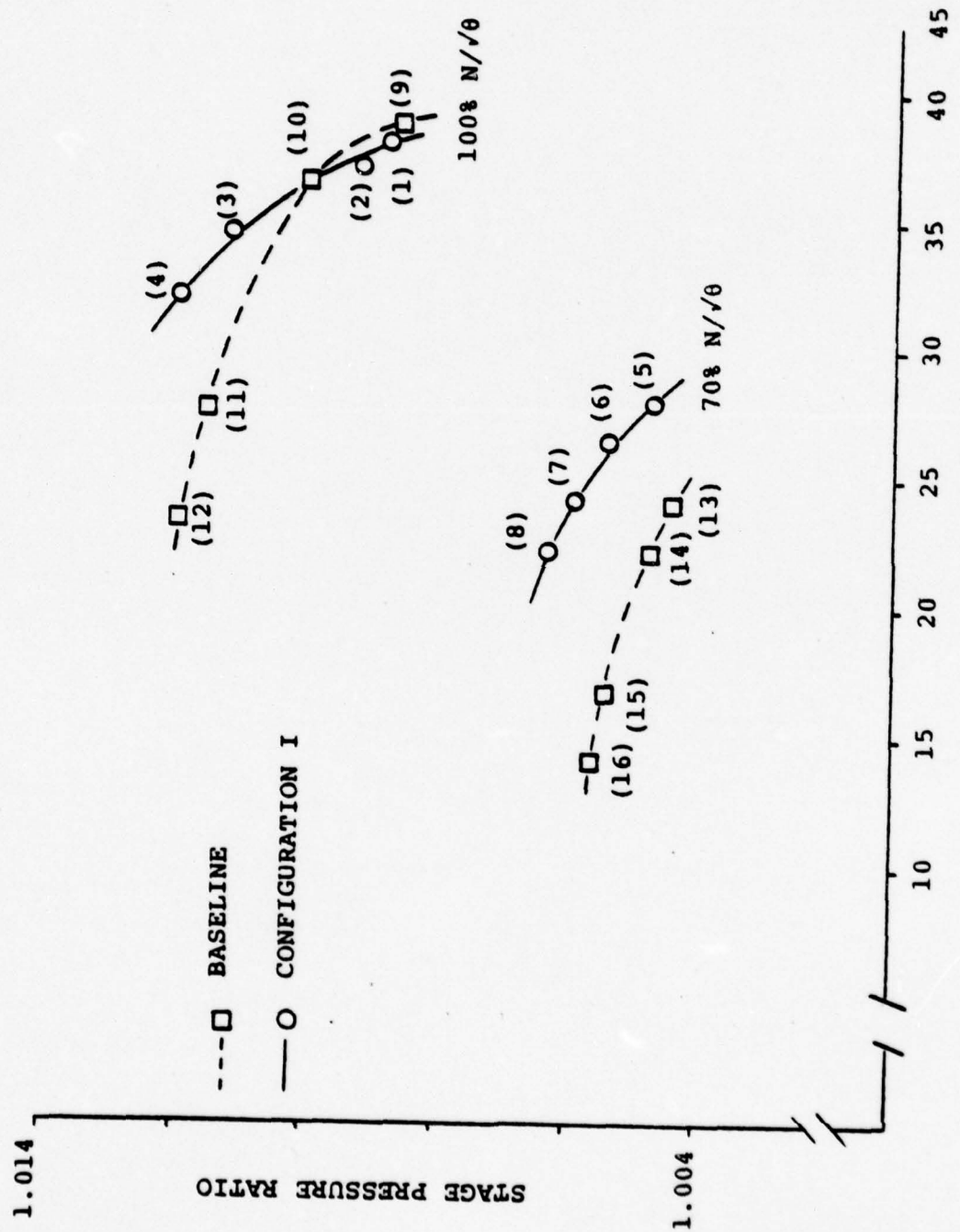
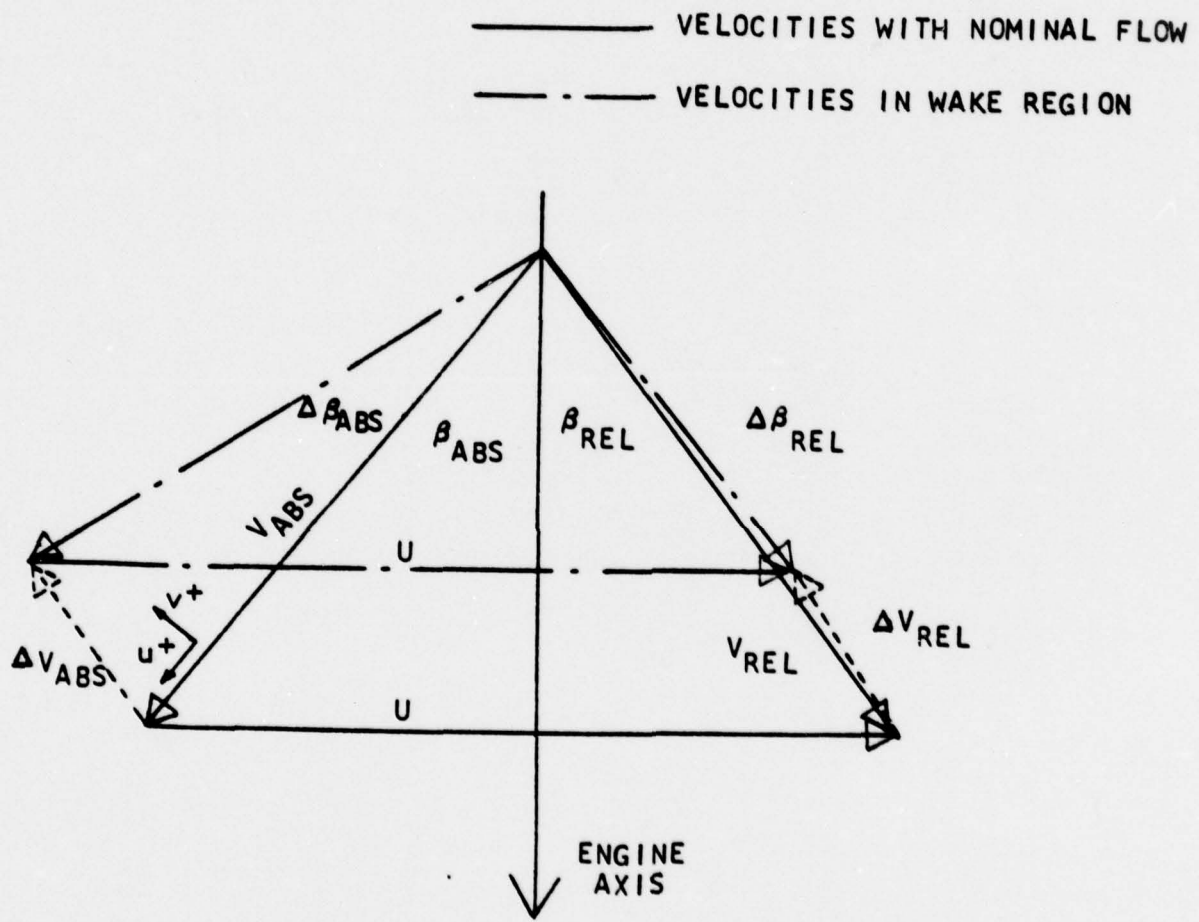


FIGURE 2. DATA POINT IDENTIFICATION IN TERMS OF  
PRESSURE RATIO AND MASS FLOW RATE



329458

FIGURE 3. REDUCTION IN RELATIVE VELOCITY GENERATED BY BLADE WAKE CREATES CORRESPONDING VELOCITY AND ANGULAR CHANGE IN ABSOLUTE FRAME

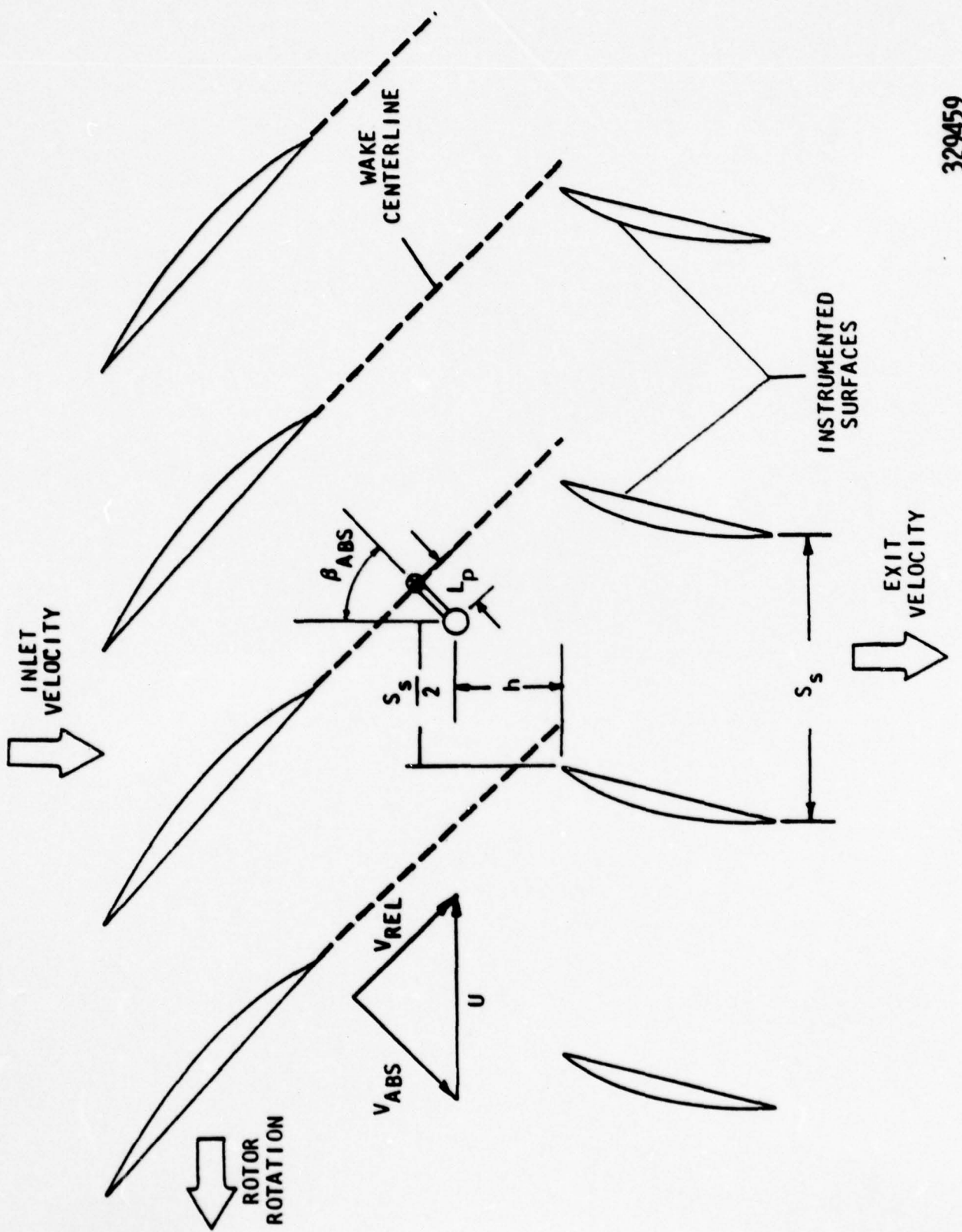


FIGURE 4. SCHEMATIC OF FLOW FIELD USED IN DYNAMIC DATA ANALYSIS

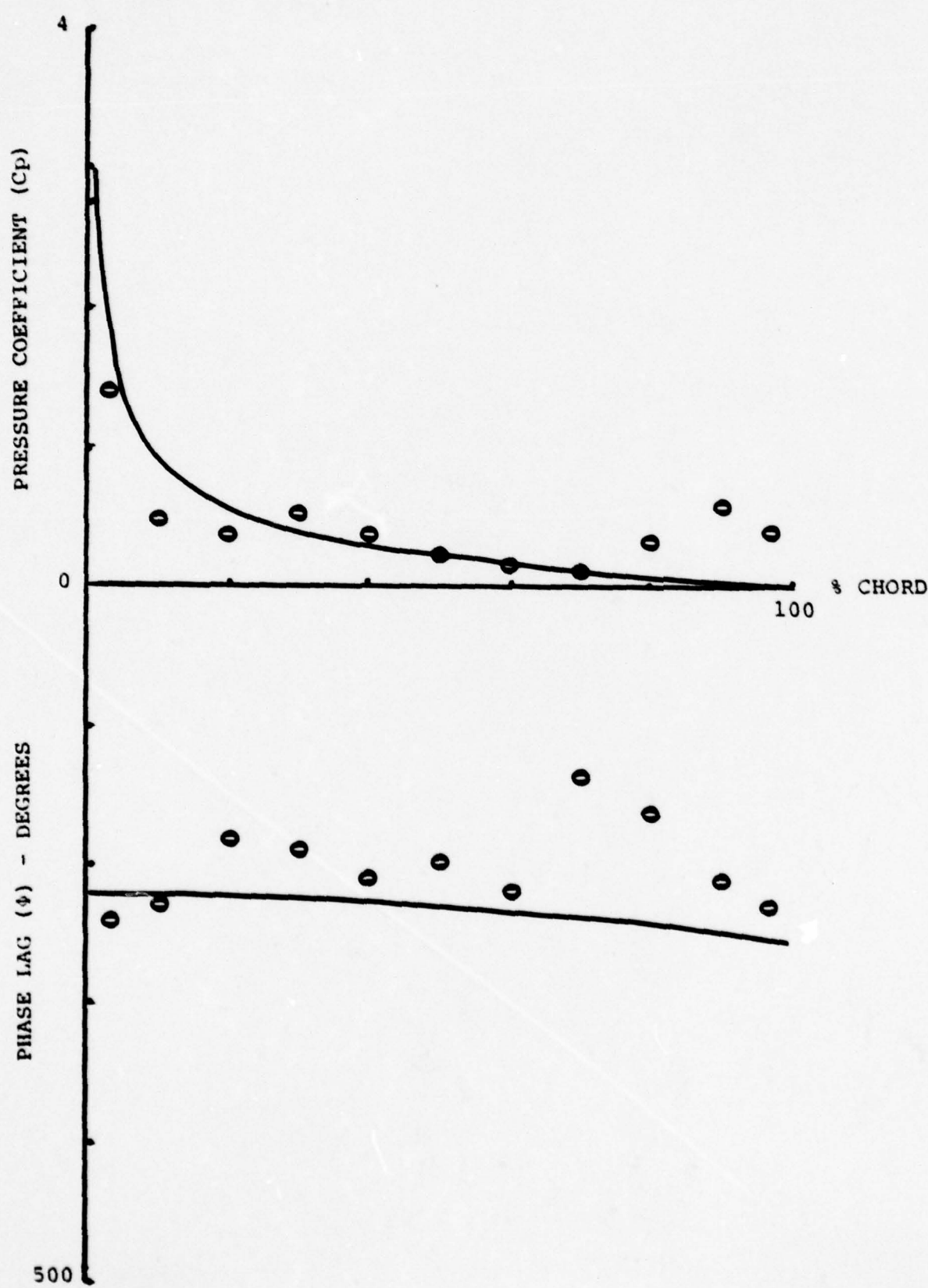


FIGURE 5. CONFIGURATION I, POINT 1, FIRST HARMONIC DATA AND PREDICTION FROM REFERENCE 4

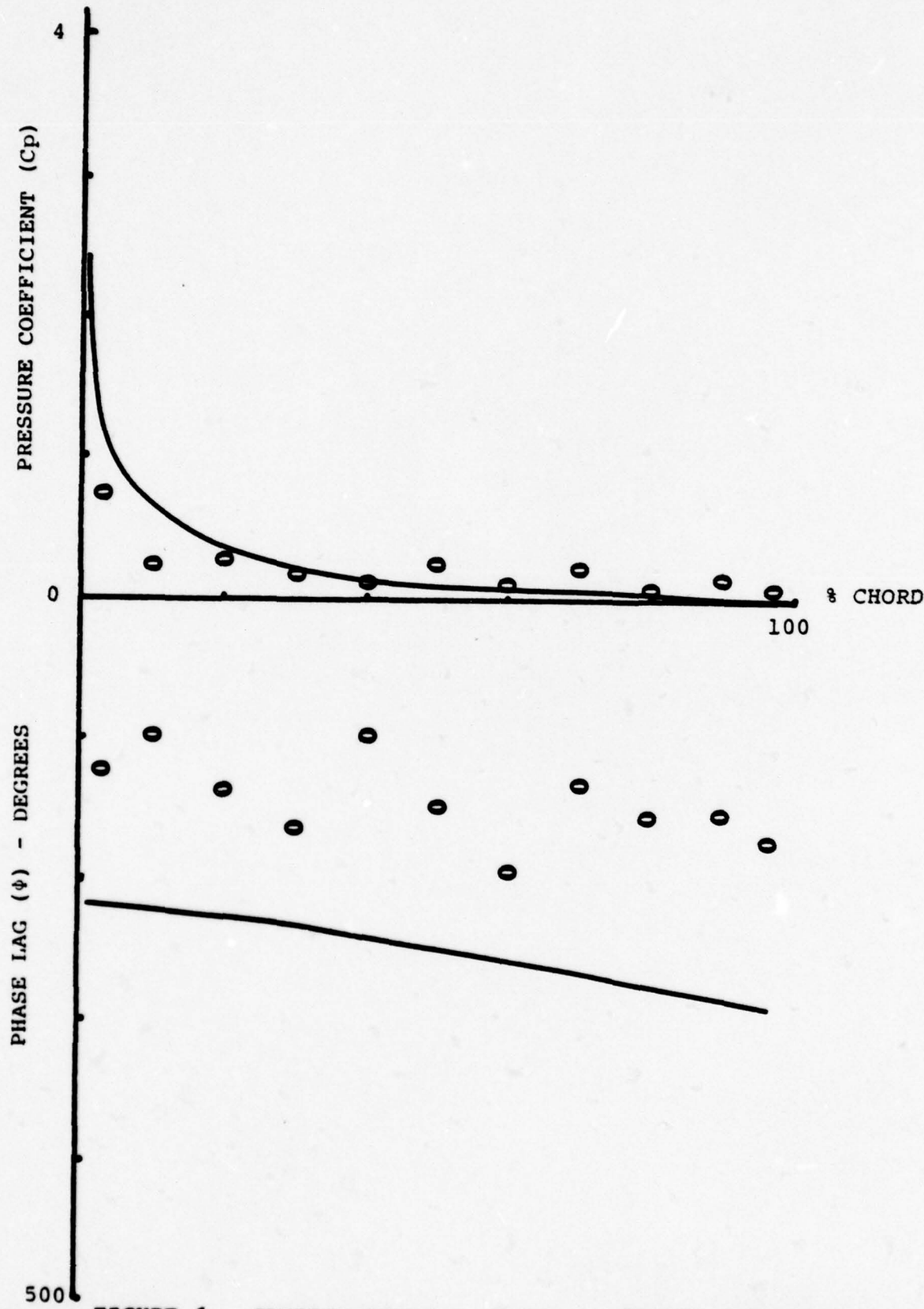


FIGURE 6. CONFIGURATION I, POINT 1, SECOND HARMONIC  
DATA AND PREDICTION FROM REFERENCE 4

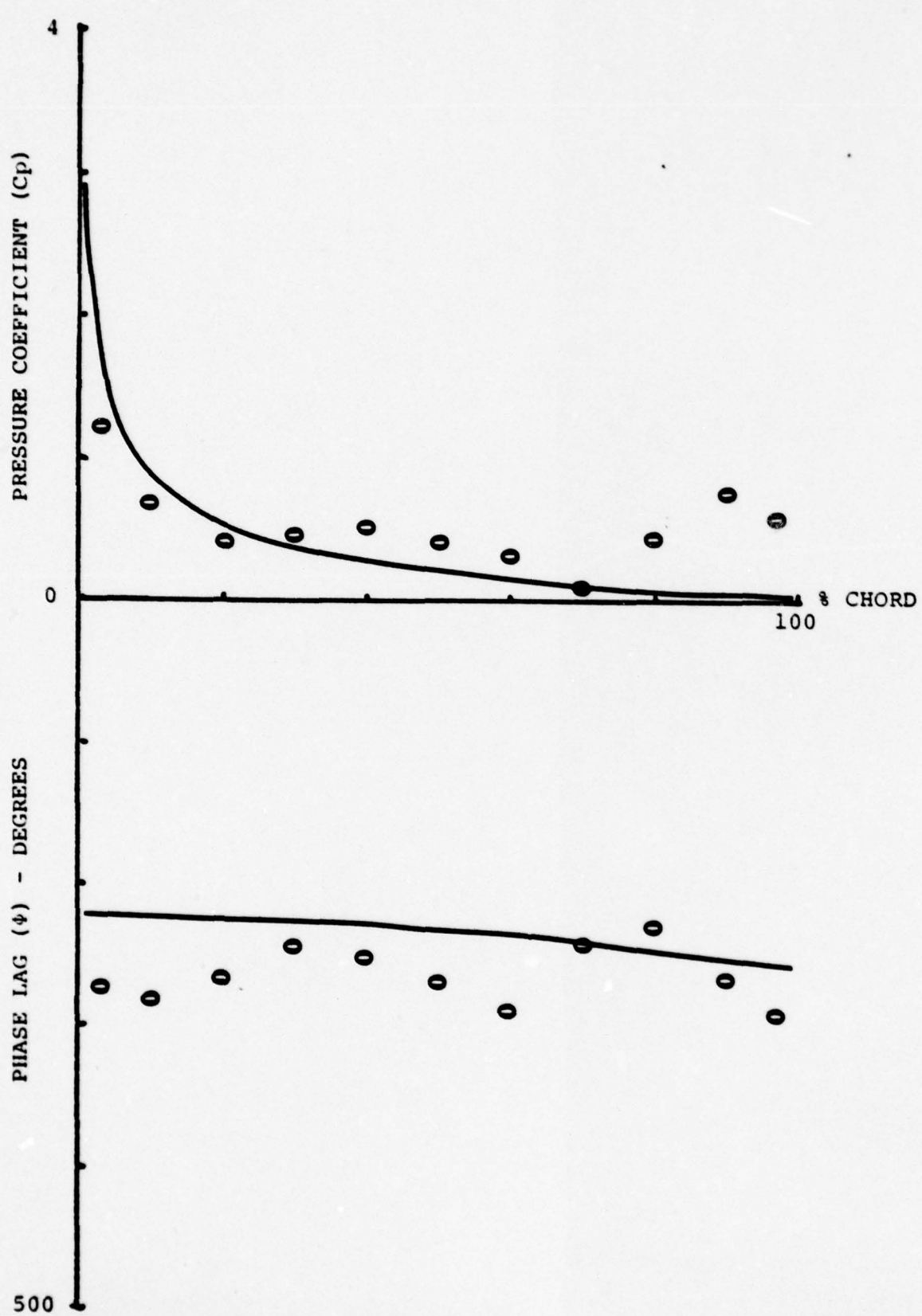


FIGURE 7. CONFIGURATION I, POINT 2, FIRST HARMONIC DATA AND PREDICTION FROM REFERENCE 4

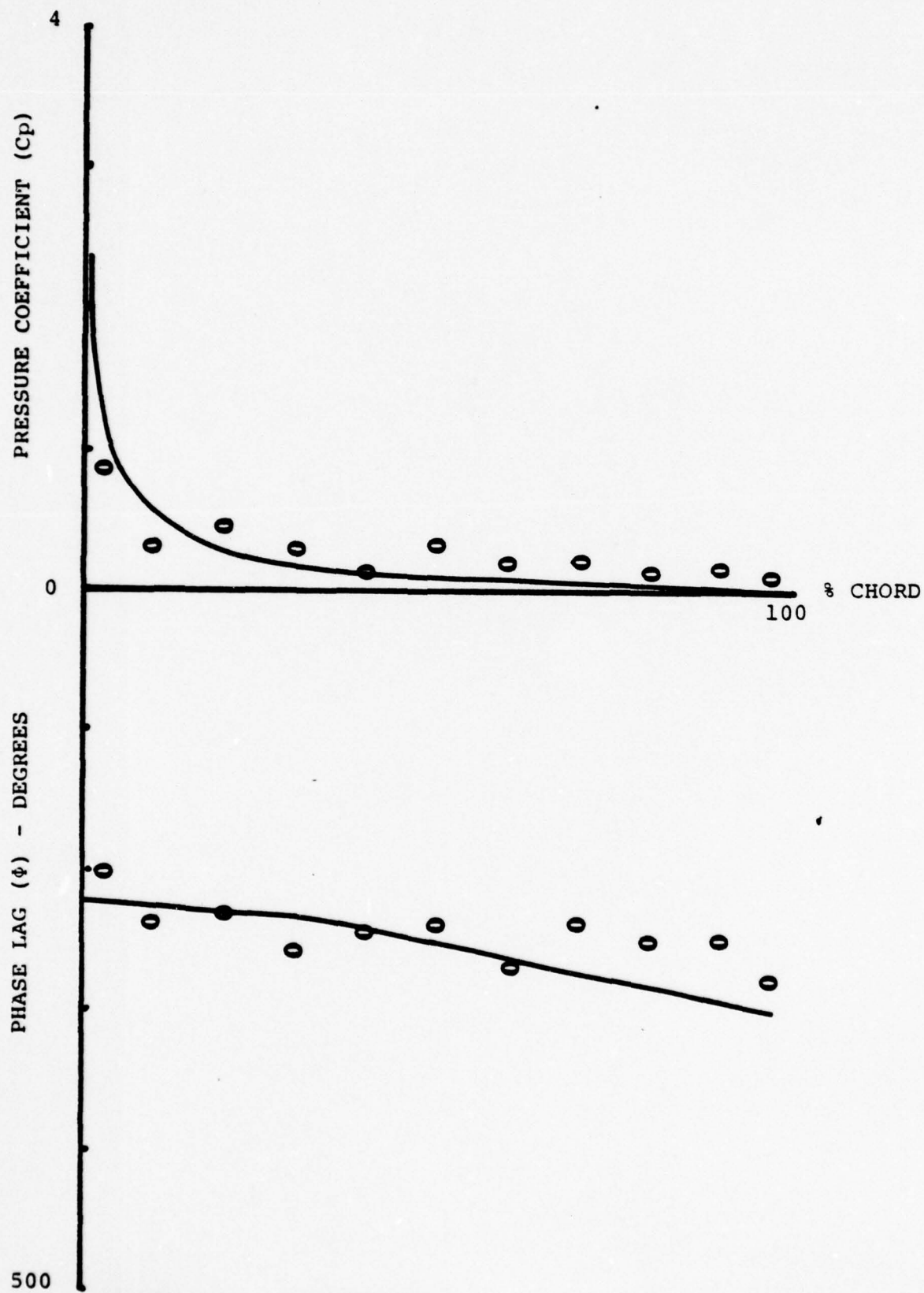


FIGURE 8. CONFIGURATION I, POINT 2, SECOND HARMONIC DATA AND PREDICTION FROM REFERENCE 4

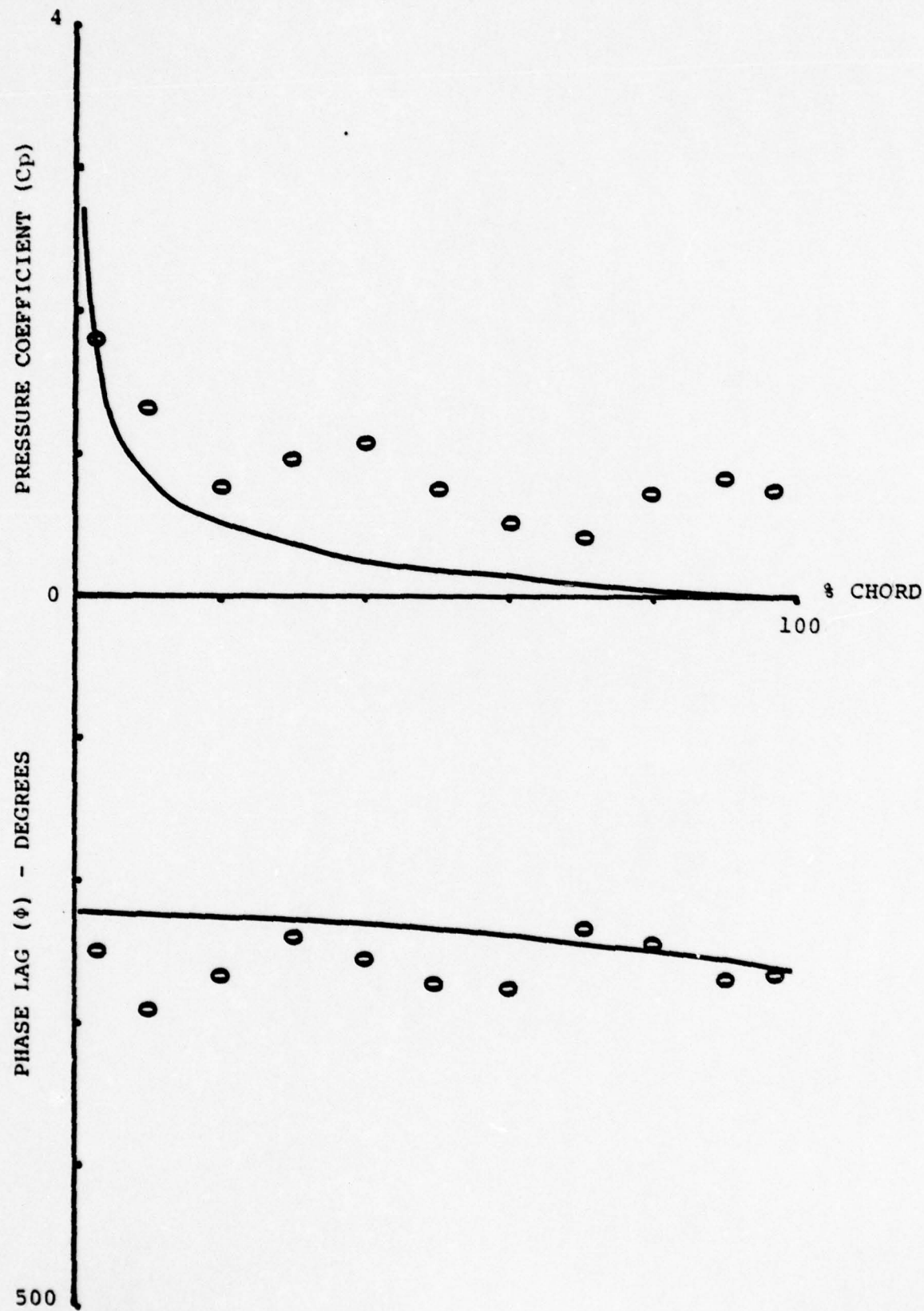


FIGURE 9. CONFIGURATION I, POINT 3, FIRST HARMONIC DATA AND PREDICTION FROM REFERENCE 4

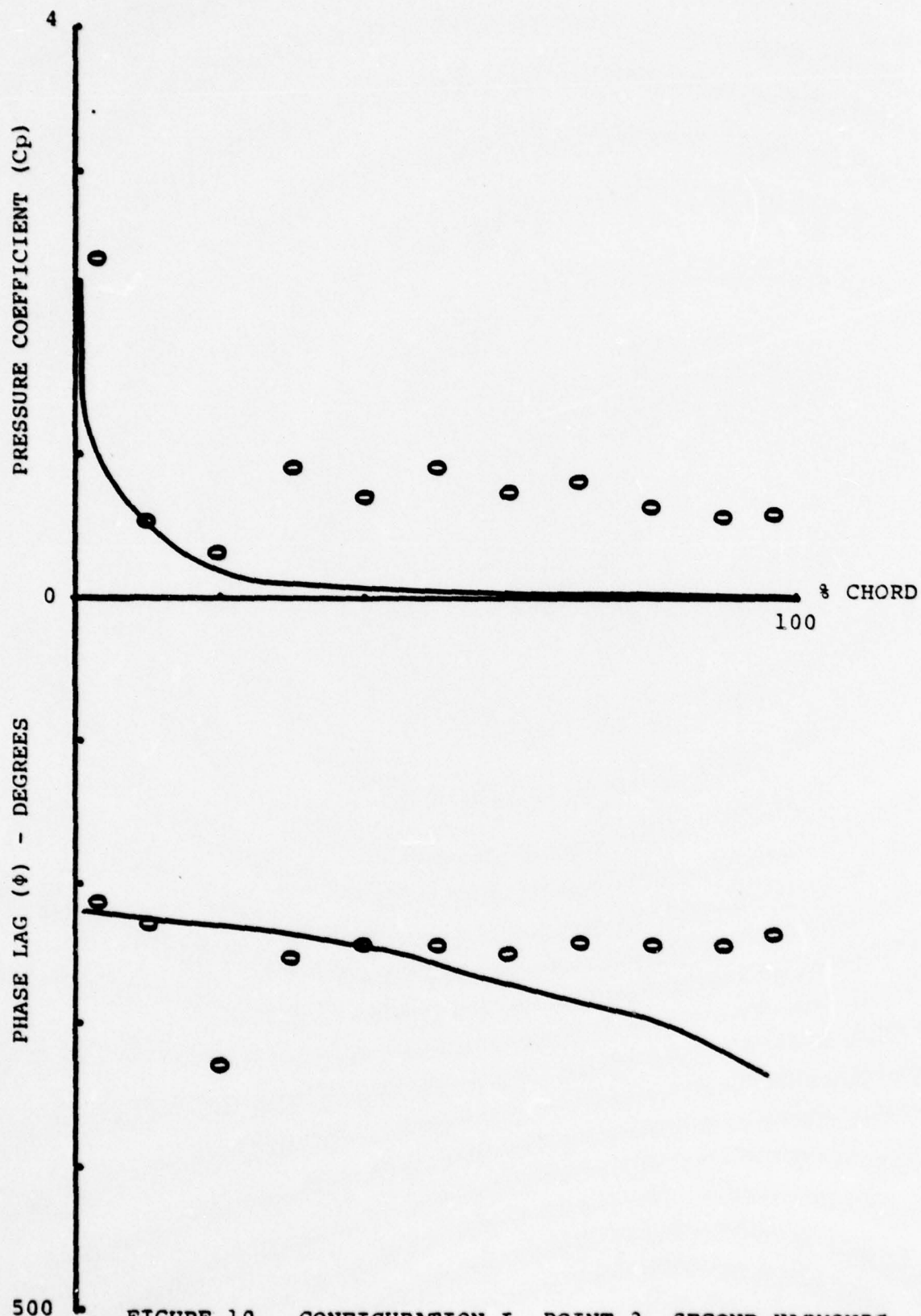


FIGURE 10. CONFIGURATION I, POINT 3, SECOND HARMONIC DATA AND PREDICTION FROM REFERENCE 4

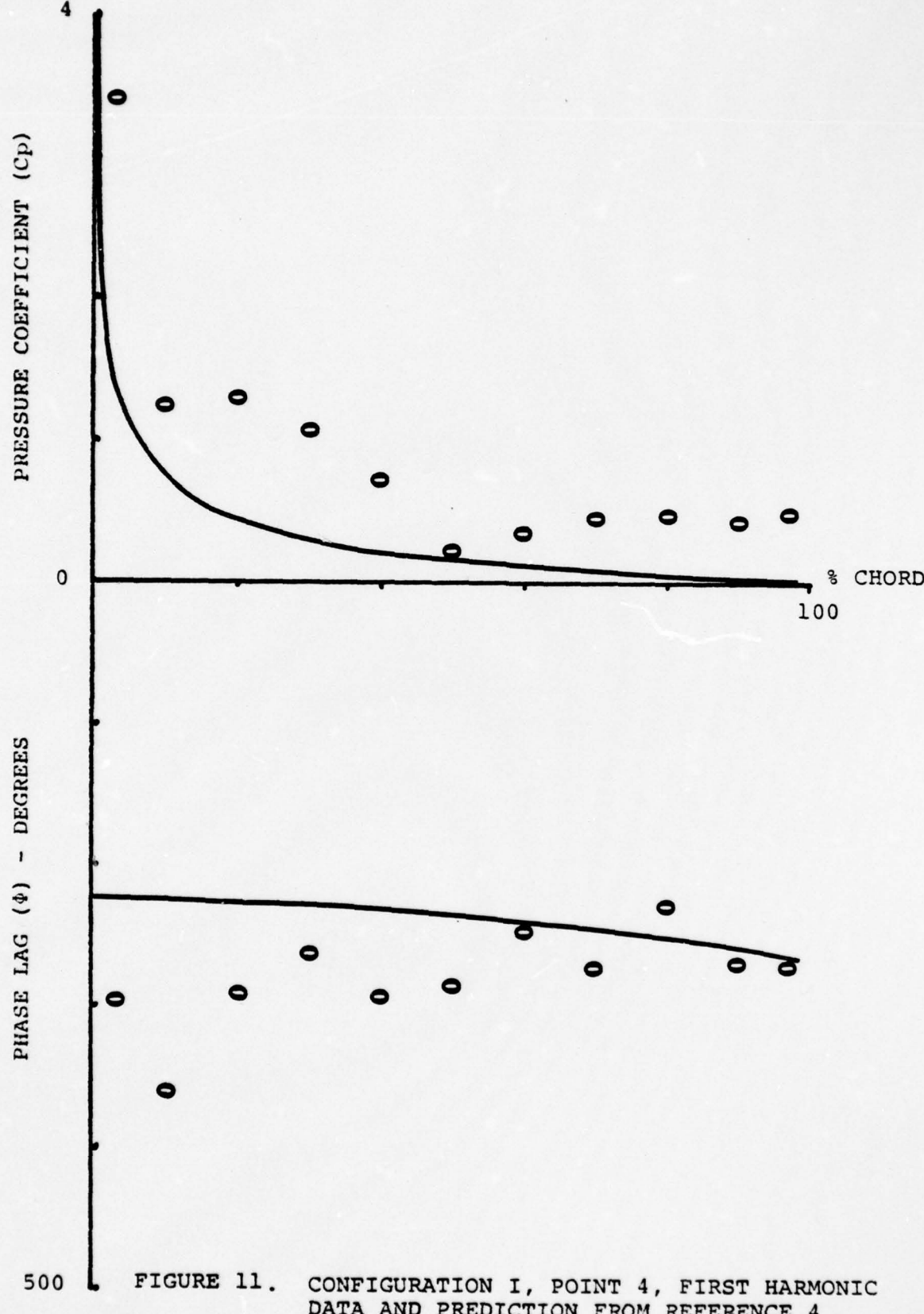


FIGURE 11. CONFIGURATION I, POINT 4, FIRST HARMONIC DATA AND PREDICTION FROM REFERENCE 4

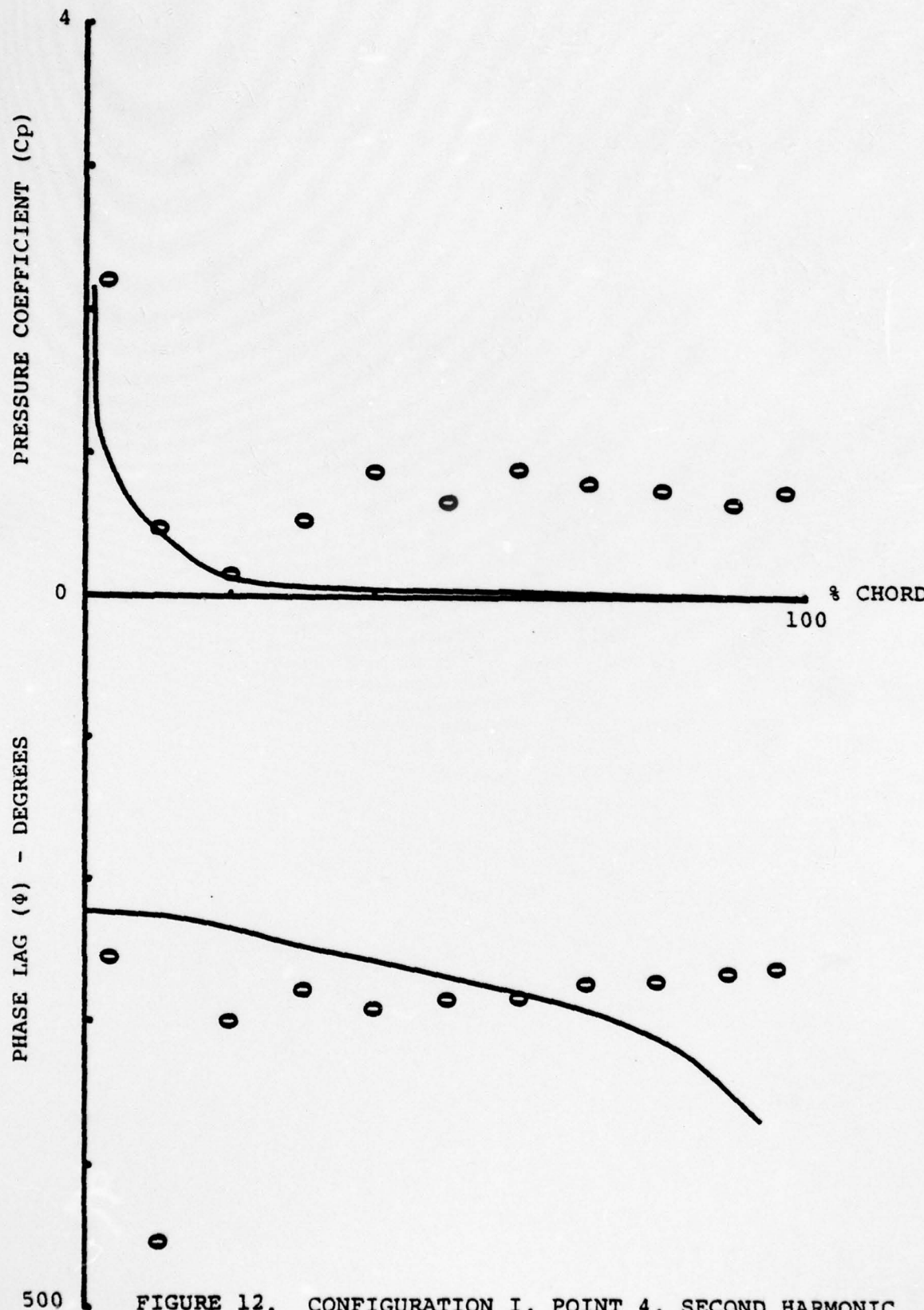


FIGURE 12. CONFIGURATION I, POINT 4, SECOND HARMONIC DATA AND PREDICTION FROM REFERENCE 4

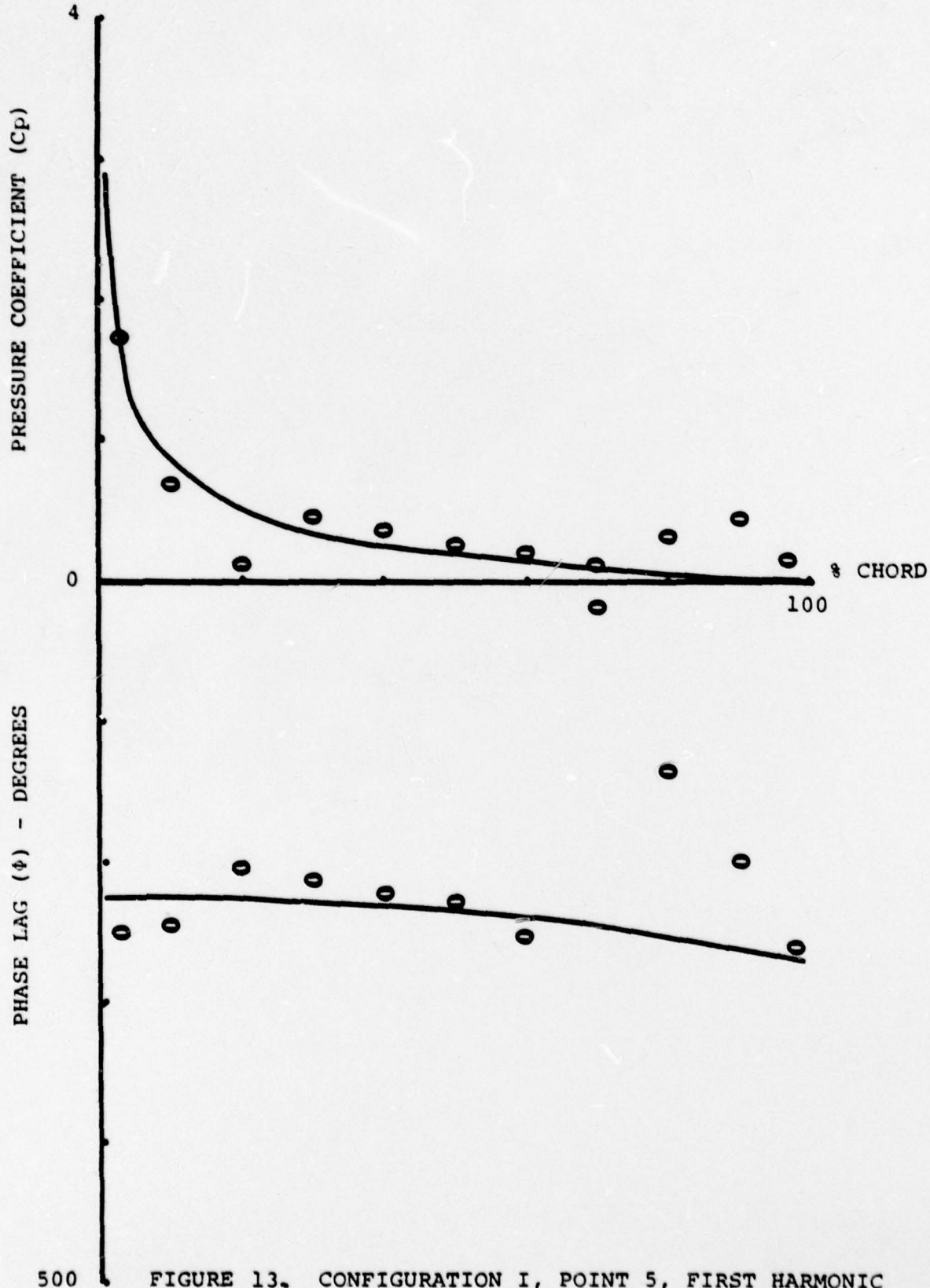


FIGURE 13. CONFIGURATION I, POINT 5, FIRST HARMONIC DATA AND PREDICTION FROM REFERENCE 4

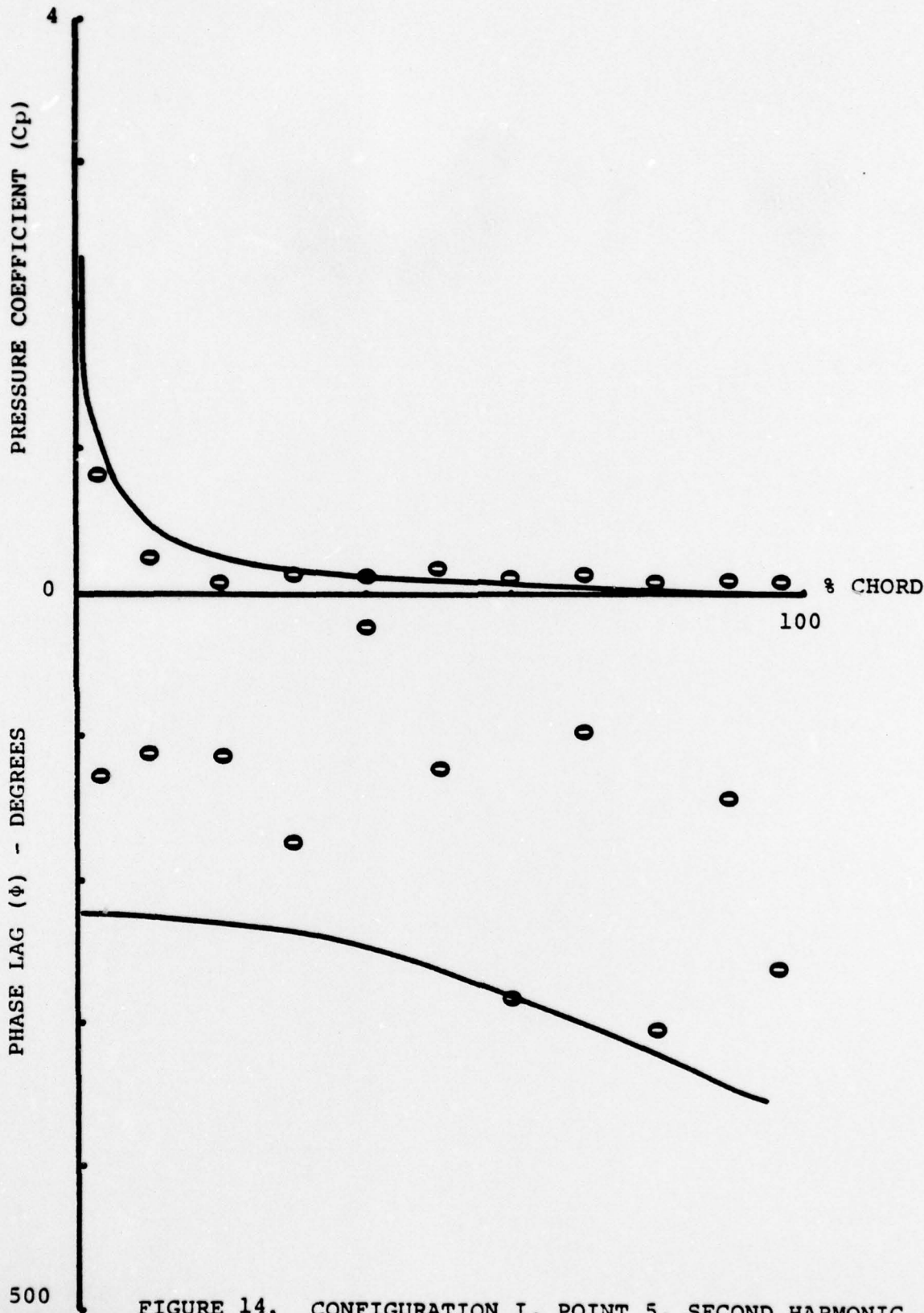


FIGURE 14. CONFIGURATION I, POINT 5, SECOND HARMONIC DATA AND PREDICTION FROM REFERENCE 4

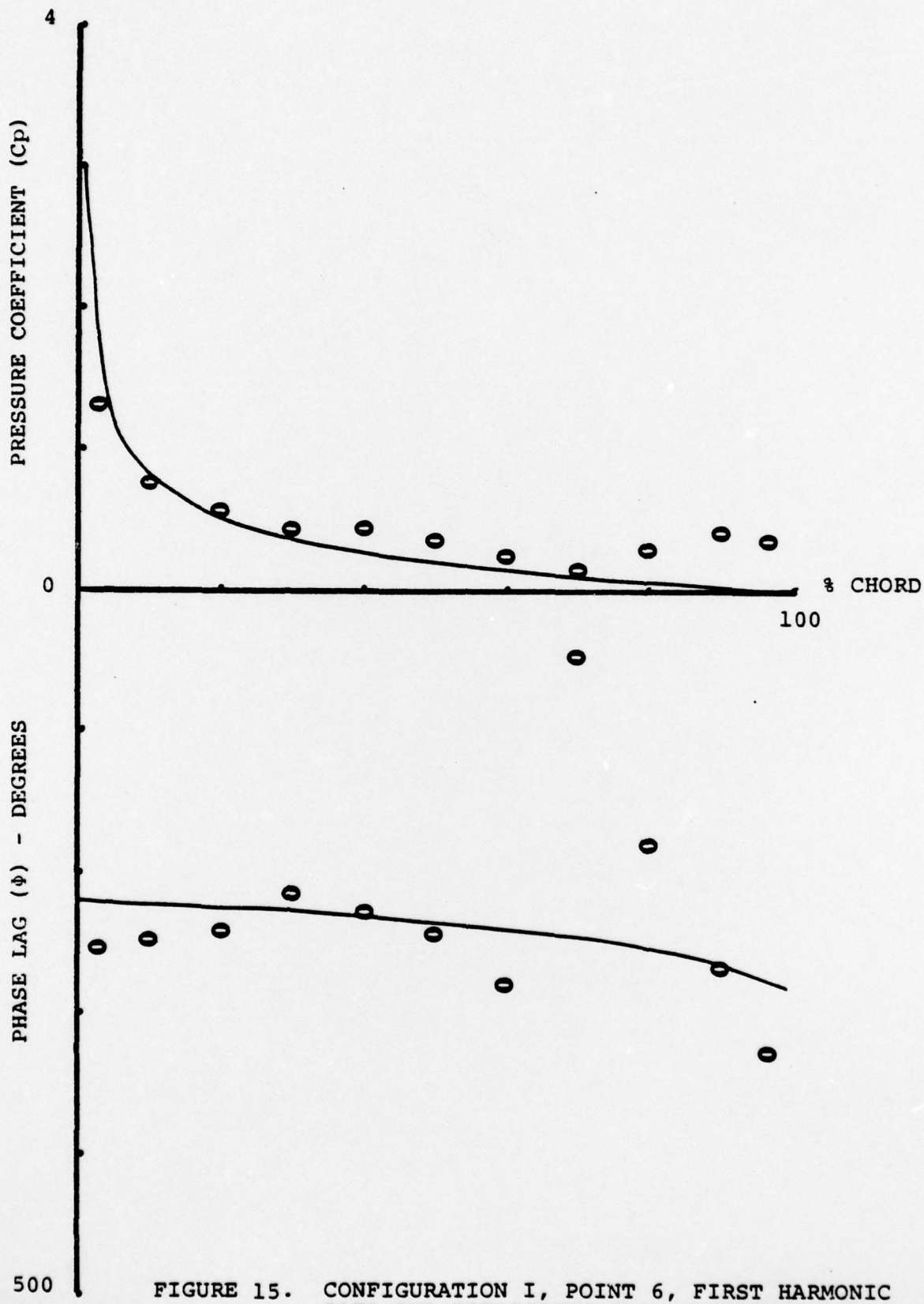


FIGURE 15. CONFIGURATION I, POINT 6, FIRST HARMONIC DATA AND PREDICTION FROM REFERENCE 4

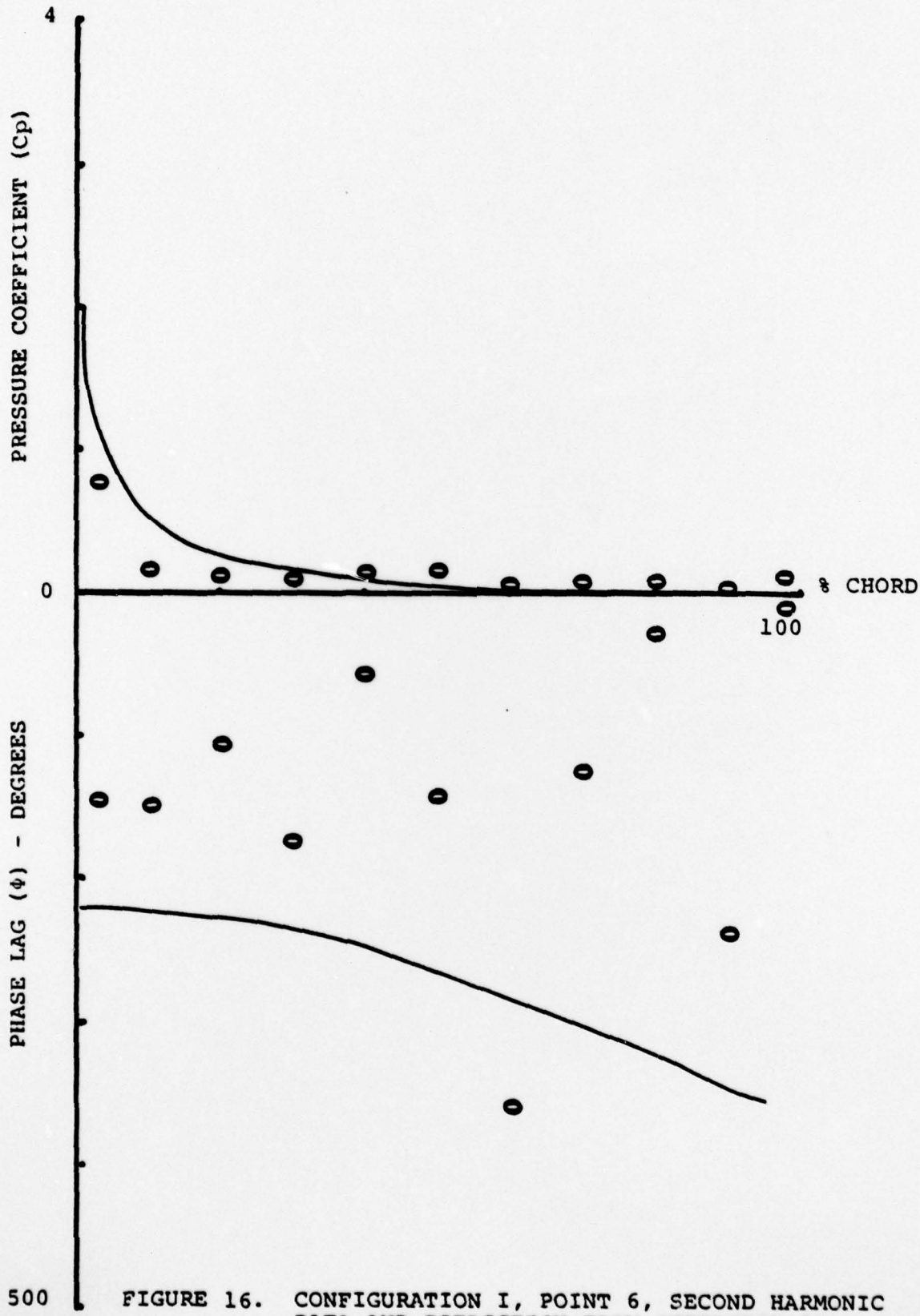


FIGURE 16. CONFIGURATION I, POINT 6, SECOND HARMONIC DATA AND PREDICTION FROM REFERENCE 4

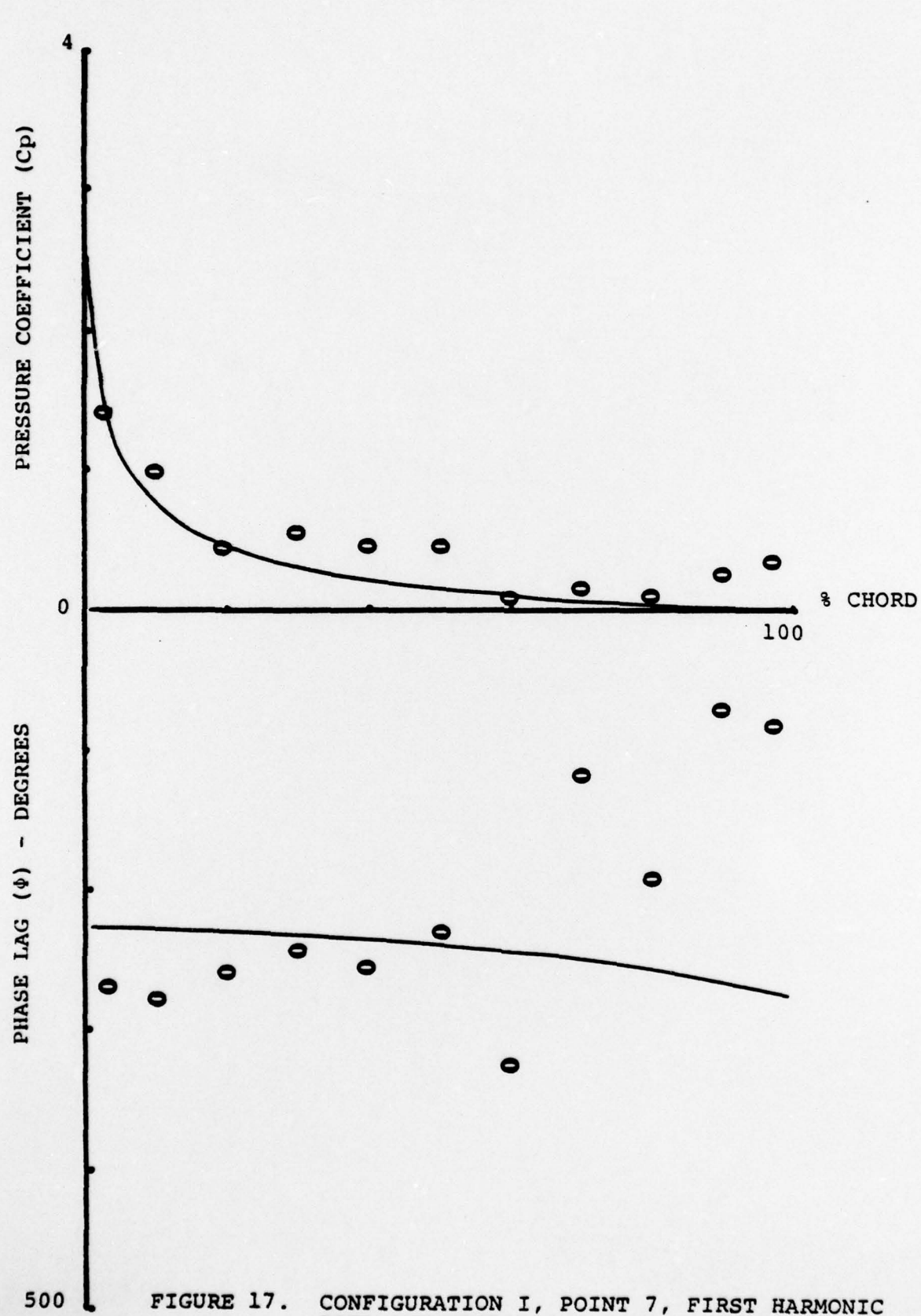


FIGURE 17. CONFIGURATION I, POINT 7, FIRST HARMONIC DATA AND PREDICTION FROM REFERENCE 4

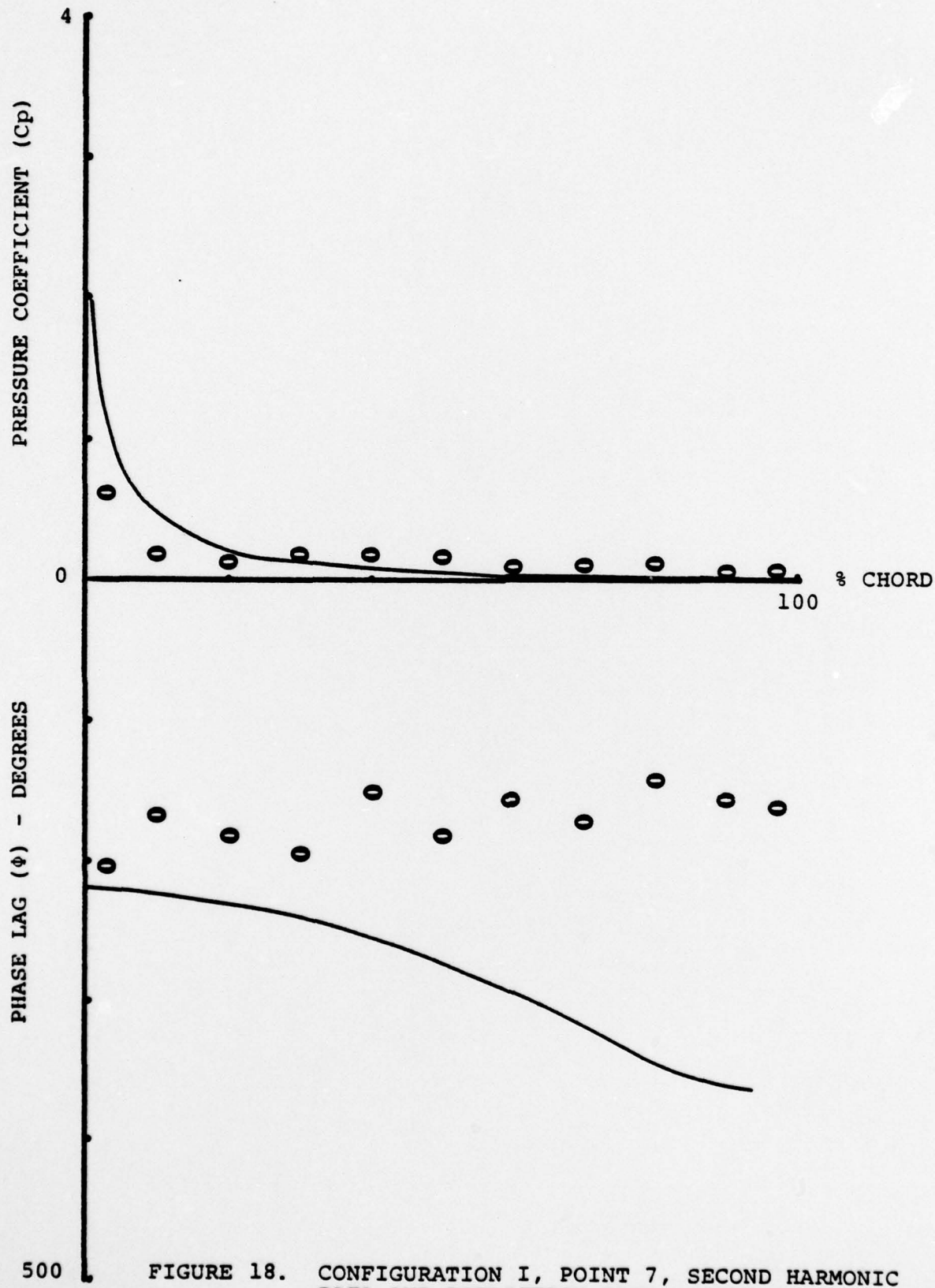


FIGURE 18. CONFIGURATION I, POINT 7, SECOND HARMONIC DATA AND PREDICTION FROM REFERENCE 4

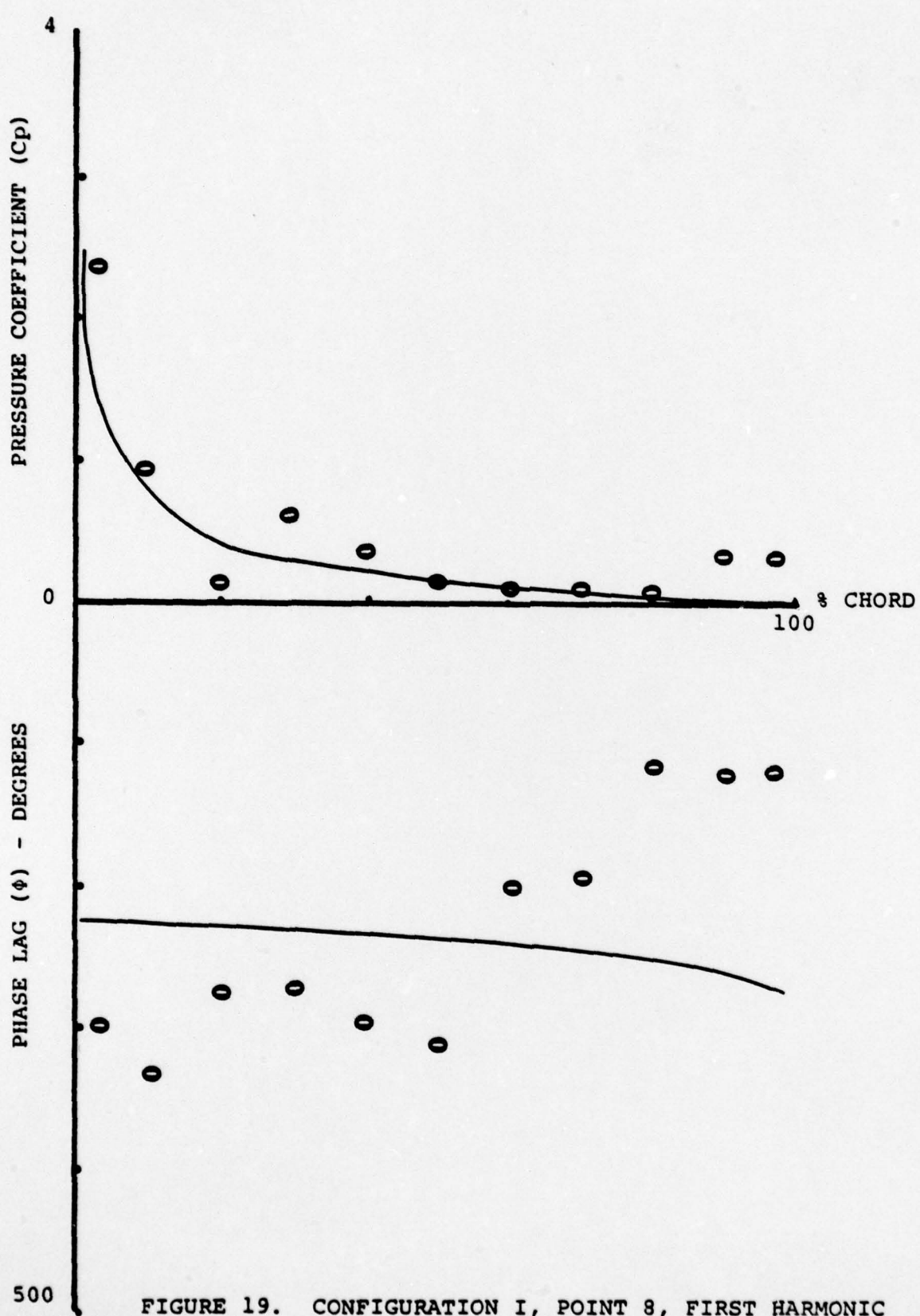


FIGURE 19. CONFIGURATION I, POINT 8, FIRST HARMONIC DATA AND PREDICTION FROM REFERENCE 4

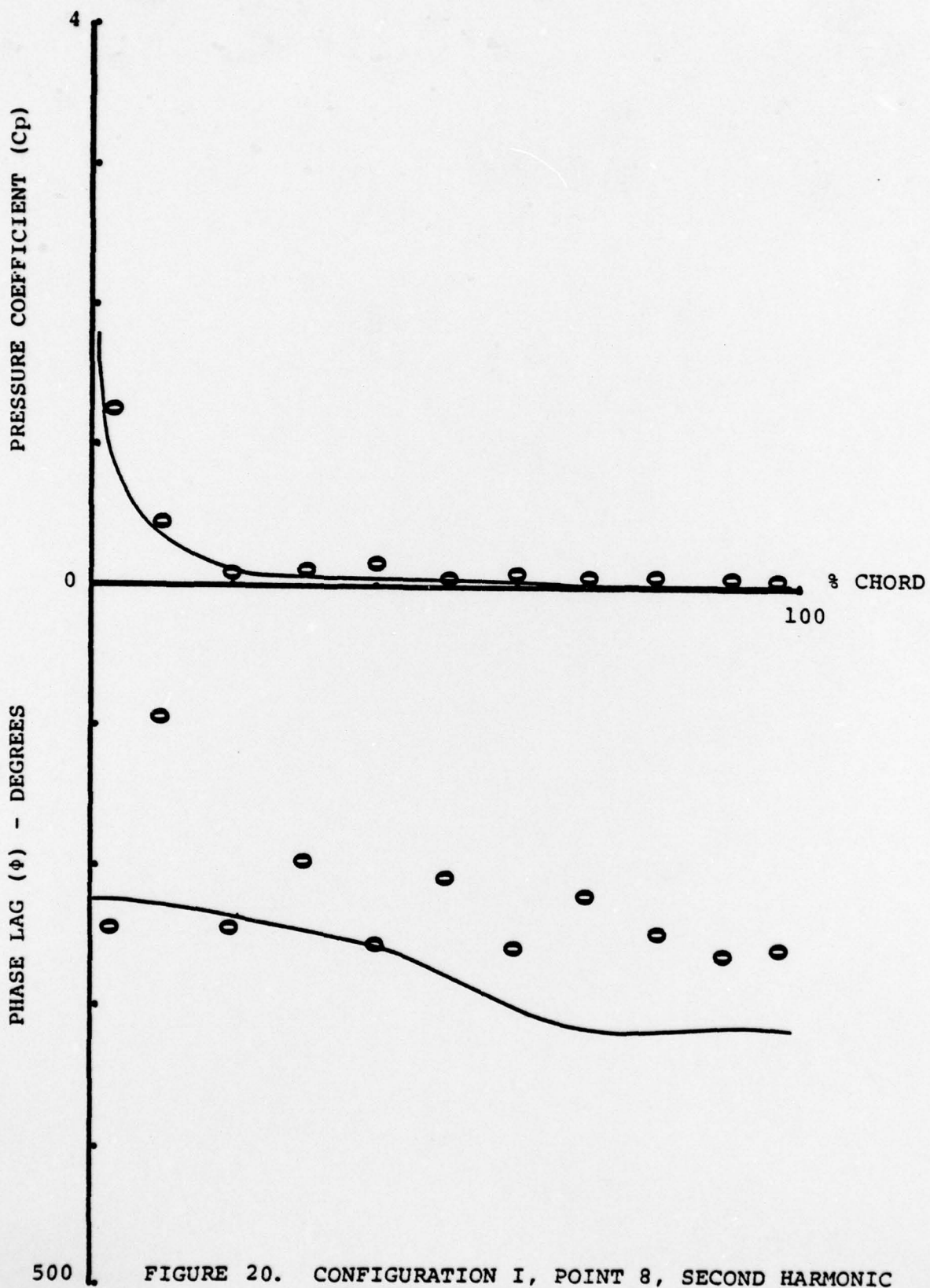
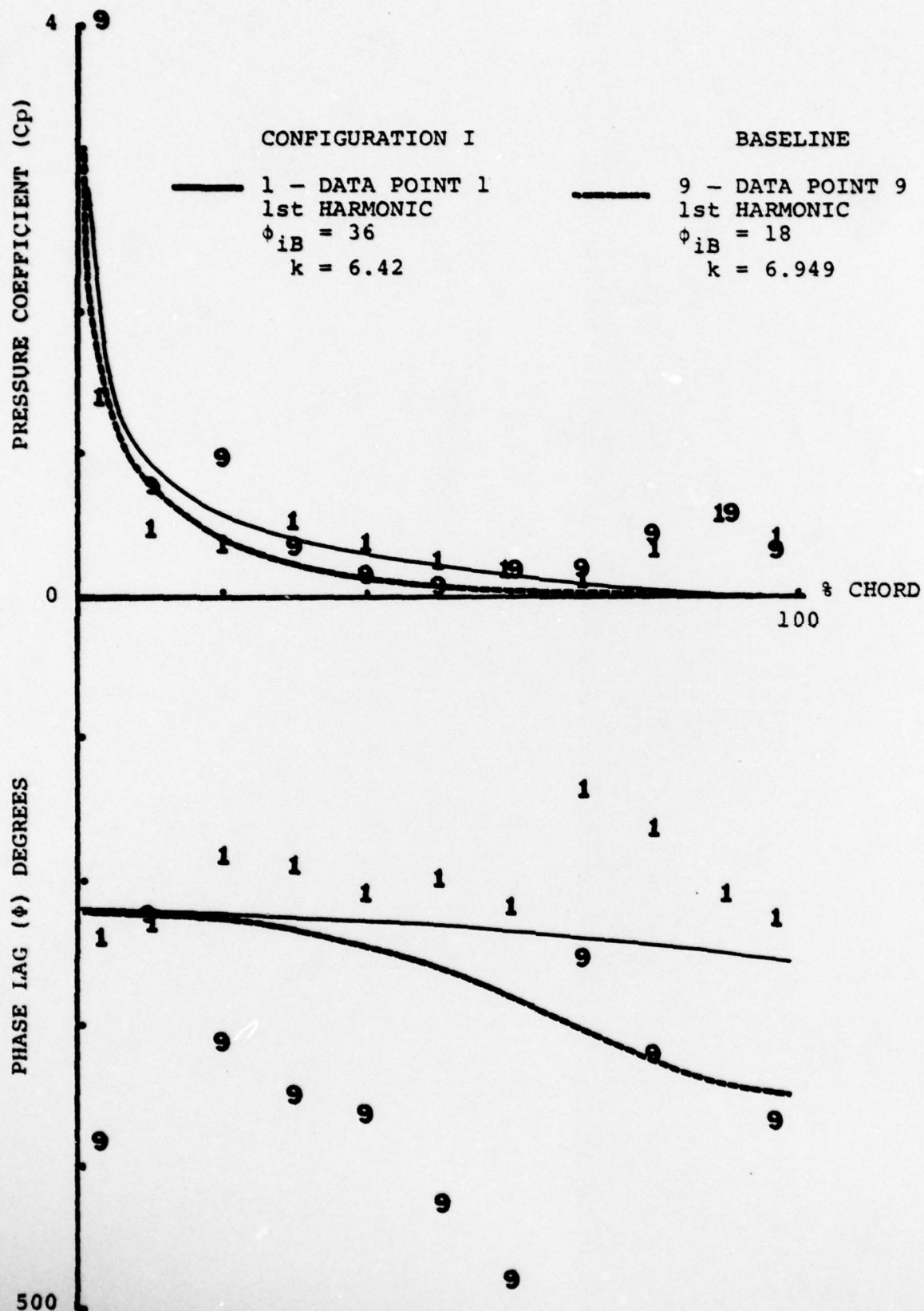


FIGURE 20. CONFIGURATION I, POINT 8, SECOND HARMONIC DATA AND PREDICTION FROM REFERENCE 4



**FIGURE 21. CONFIGURATION I - BASELINE COMPARISON AND PREDICTION FROM REFERENCE 4**

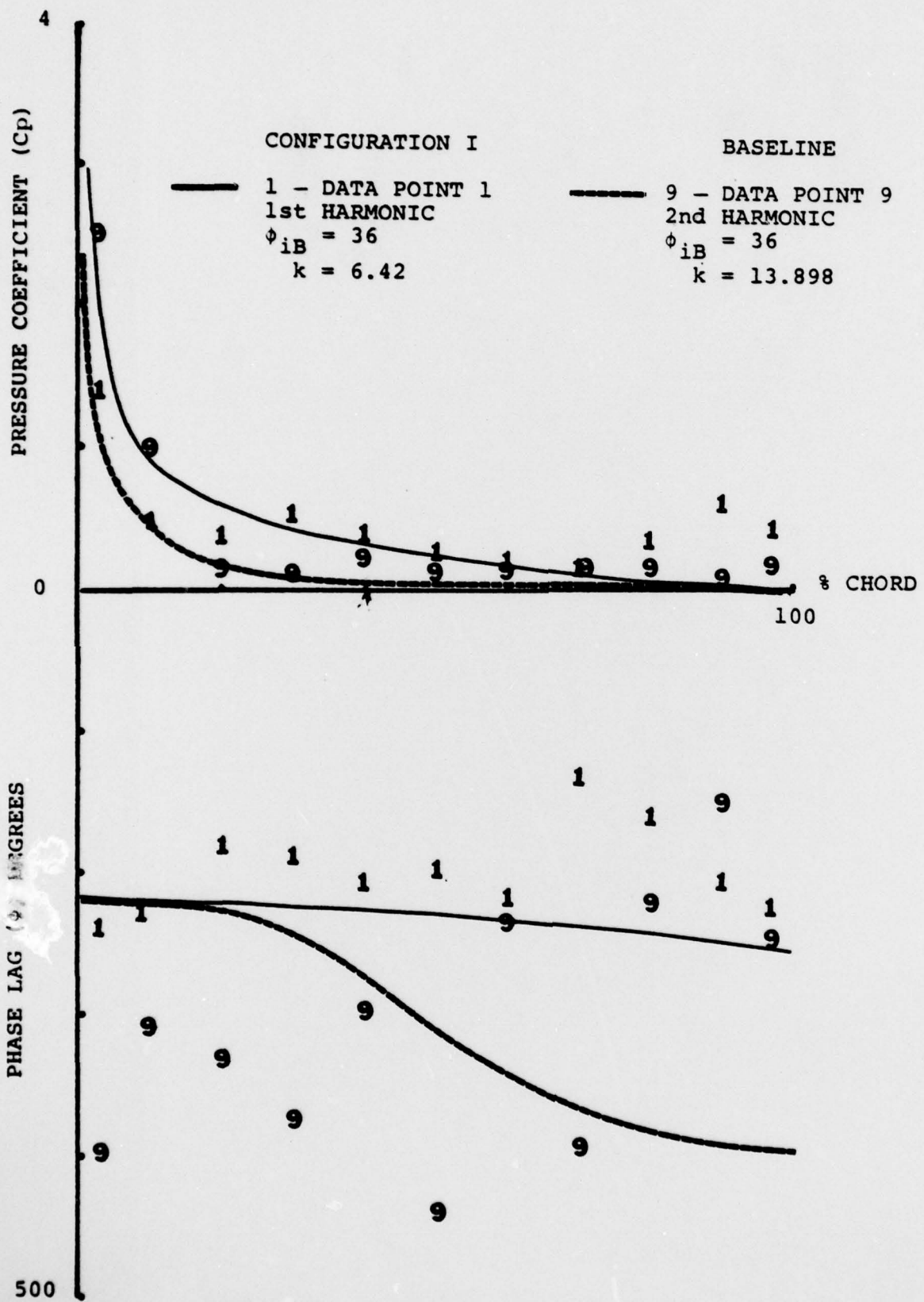


FIGURE 22. CONFIGURATION I - BASELINE COMPARISON AND PREDICTION FROM REFERENCE 4

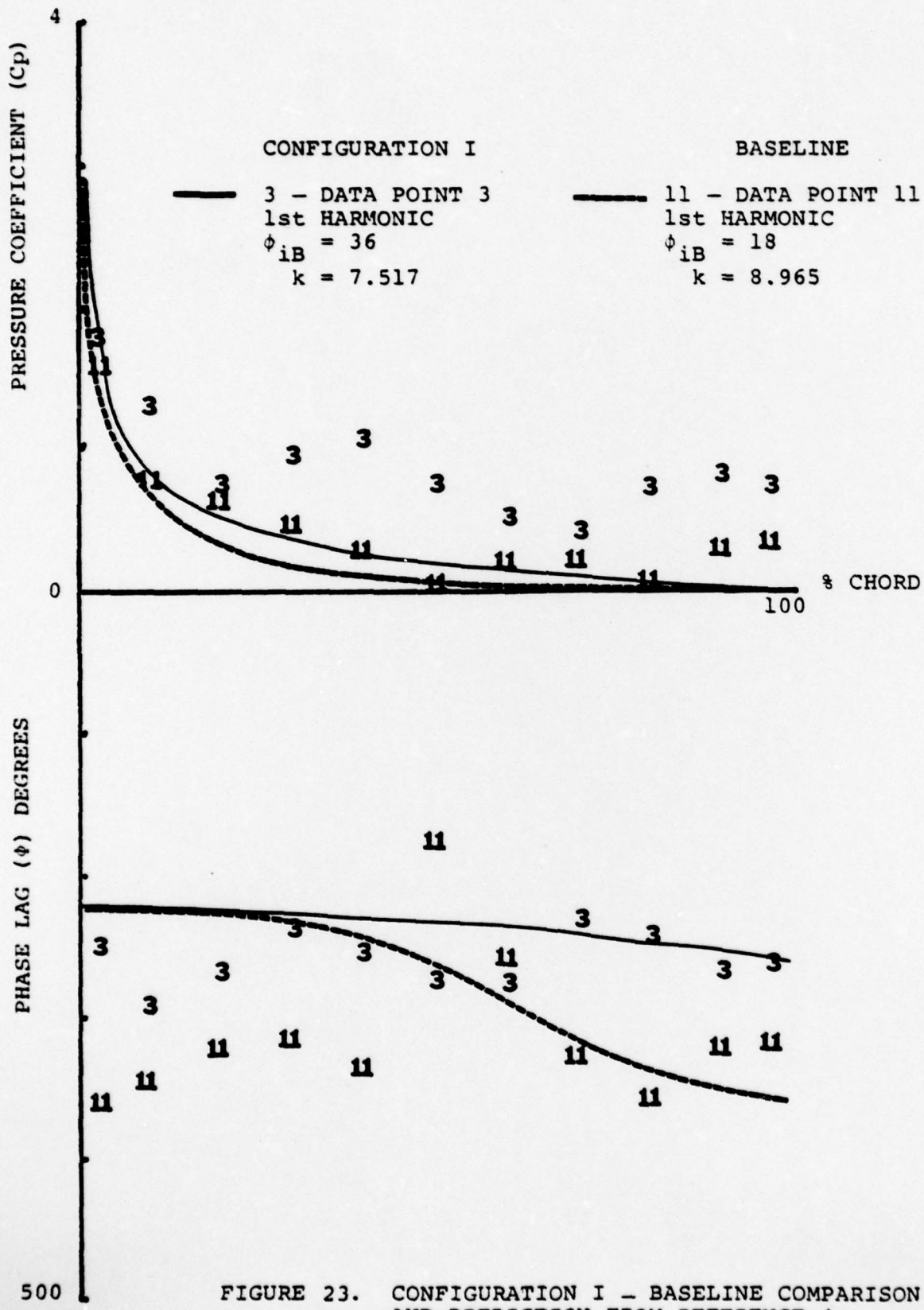


FIGURE 23. CONFIGURATION I - BASELINE COMPARISON AND PREDICTION FROM REFERENCE 4

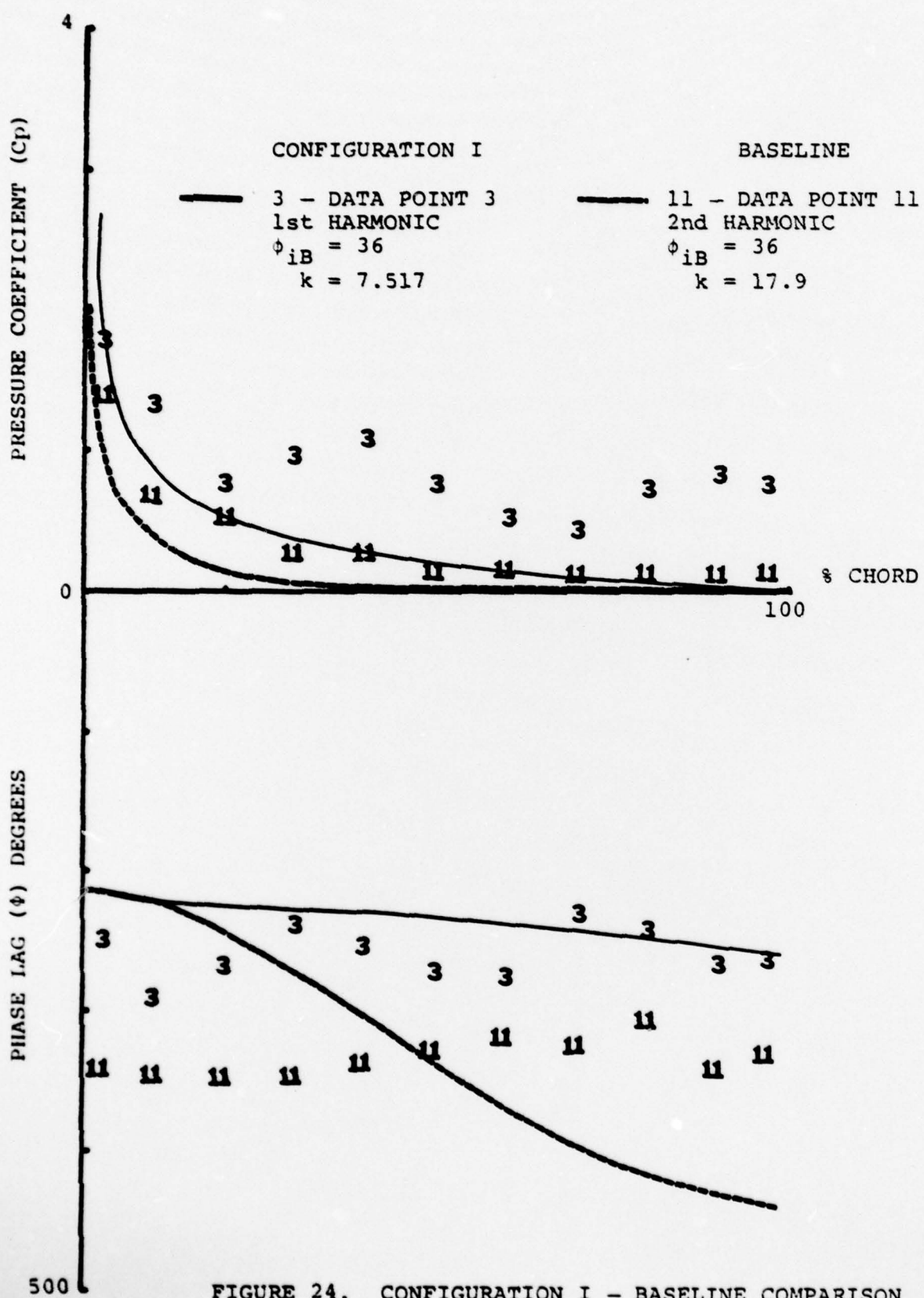


FIGURE 24. CONFIGURATION I - BASELINE COMPARISON AND PREDICTION FROM REFERENCE 4

## UNCLASSIFIED

SECURITY CLASSIFICATION OF THIS PAGE (When Data Entered)

| REPORT DOCUMENTATION PAGE   |                       | READ INSTRUCTIONS BEFORE COMPLETING FORM  |
|---|-----------------------|---|
| 1. REPORT NUMBER  | 2. GOVT ACCESSION NO. | 3. RECIPIENT'S CATALOG NUMBER   |
| 4. TITLE (and Subtitle)<br>THE EFFECT OF INTERBLADE PHASE ANGLE AND SOLIDITY ON THE TIME-VARIANT AERODYNAMIC RESPONSE OF A COMPRESSOR STATOR  |                       | 5. TYPE OF REPORT & PERIOD COVERED<br>Annual Technical<br>1978 May 01 - 1979 May 01 |
| 7. AUTHOR(s)<br>R. R. Allran  |                       | 6. PERFORMING ORG. REPORT NUMBER<br>DDA EDR 9930                                    |
| 9. PERFORMING ORGANIZATION NAME AND ADDRESS<br>Detroit Diesel Allison<br>P.O. Box 894, Indianapolis, IN 46206   |                       | 10. PROGRAM ELEMENT, PROJECT, TASK AREA & WORK UNIT NUMBERS                         |
| 11. CONTROLLING OFFICE NAME AND ADDRESS<br>Air Force Office of Scientific Research<br>Building 410<br>Bolling Air Force Base, D.C. 20332  |                       | 12. REPORT DATE<br>June 1979  |
| 14. MONITORING AGENCY NAME & ADDRESS(if different from Controlling Office)  |                       | 13. NUMBER OF PAGES<br>51   |
|   |                       | 15. SECURITY CLASS. (of this report)<br>Unclassified                                |
|   |                       | 15a. DECLASSIFICATION/DOWNGRADING SCHEDULE  |
| 16. DISTRIBUTION STATEMENT (of this Report)<br><br>Approved for public release; distribution unlimited.   |                       |   |
| 17. DISTRIBUTION STATEMENT (of the abstract entered in Block 20, if different from Report)  |                       |   |
| 18. SUPPLEMENTARY NOTES   |                       |   |
| 19. KEY WORDS (Continue on reverse side if necessary and identify by block number)<br><br>Turbomachinery, Compressors, Unsteady Aerodynamics, Forced Vibrations   |                       |   |
| 20. ABSTRACT (Continue on reverse side if necessary and identify by block number)<br><br>→ The overall objective of this experimental program was to quantify the effects of the reduced frequency as well as the interblade phase angle and associated solidity variations on the fundamental time-variant aerodynamics relevant to forced response in turbomachinery. This was accomplished in a large, low speed, single-stage research compressor which permitted variation of the interblade phase angle and solidity by varying the number of rotor to stator blades. |                       |   |

**UNCLASSIFIED**

SECURITY CLASSIFICATION OF THIS PAGE(When Data Entered)

> A single value of interblade phase angle, 36 degrees and a corresponding value of solidity of .758, the aerodynamically induced fluctuating surface pressure distributions on the downstream vane row, with the primary source of excitation being the upstream rotor wakes, were measured over a wide range of compressor operating conditions.

The individual vane surface data were investigated to determine the effect of interblade phase angle and solidity on the overall unsteady pressure magnitude as well as to determine the dynamic pressure coefficient and aero-dynamic phase lag for the unsteady pressure differential across the vanes. The unsteady pressure differential data were correlated with predictions from a state-of-the-art flat plate cascade transverse gust analysis.

**UNCLASSIFIED**

SECURITY CLASSIFICATION OF THIS PAGE(When Data Entered)